FALL / WINTER 2025
VOLUME 17, NUMBER 2

Print ISSN: 2152-4157
Online ISSN: 2152-4165

WWW.IJERI.ORG

International Journal of Engineering Research & Innovation

Editor-in-Chief: Mark Rajai, Ph.D.
California State University Northridge

Published by the
International Association of Journals & Conferences

CUTTING EDGE JOURNAL OF RESEARCH AND INNOVATION IN ENGINEERING

www.ijeri.org

Print ISSN: 2152-4157
Online ISSN: 2152-4165

www.iajc.org

INTERNATIONAL JOURNAL OF ENGINEERING RESEARCH AND INNOVATION

ABOUT IJERI:

- IJERI is the second official journal of the International Association of Journals and Conferences (IAJC).
- IJERI is a high-quality, independent journal steered by a distinguished board of directors and supported by an international review board representing many well-known universities, colleges, and corporations in the U.S. and abroad.
- IJERI has an impact factor of **1.58**, placing it among an elite group of most-cited engineering journals worldwide.

OTHER IAJC JOURNALS:

- The International Journal of Modern Engineering (IJME) For more information visit www.ijme.us
- The Technology Interface International Journal (TIIJ) For more information visit www.tiij.org

IJERI SUBMISSIONS:

- Manuscripts should be sent electronically to the manuscript editor, Dr. Philip Weinsier, at philipw@bgsu.edu.

  For submission guidelines visit www.ijeri.org/submissions

TO JOIN THE REVIEW BOARD:

- Contact the chair of the International Review Board, Dr. Philip Weinsier, at philipw@bgsu.edu.

  For more information visit www.ijeri.org/editorial

INDEXING ORGANIZATIONS:

- IJERI is indexed by numerous agencies. For a complete listing, please visit us at www.ijeri.org.

Contact us:

Mark Rajai, Ph.D.

Editor-in-Chief
California State University-Northridge
College of Engineering and Computer Science
Room: JD 4510
Northridge, CA 91330
Office: (818) 677-5003
Email: mrajai@csun.edu

www.tiij.org

www.ijme.us

International Journal of Engineering Research and Innovation

The INTERNATIONAL JOURNAL OF ENGINEERING RESEARCH AND INNOVATION (IJERI) is an independent and not-for-profit publication, which aims to provide the engineering community with a resource and forum for scholarly expression and reflection.

IJERI is published twice annually (fall and spring issues) and includes peer-reviewed research articles, editorials, and commentary that contribute to our understanding of the issues, problems, and research associated with engineering and related fields. The journal encourages the submission of manuscripts from private, public, and academic sectors. The views expressed are those of the authors and do not necessarily reflect the opinions of the IJERI editors.

EDITORIAL OFFICE:

Mark Rajai, Ph.D.
Editor-in-Chief
Office: (818) 677-2167
Email: ijmeeditor@iajc.org
Dept. of Manufacturing Systems Engineering & Management
California State University-Northridge
18111 Nordhoff Street
Northridge, CA 91330-8332

The International Journal of Engineering Research and Innovation Editors

Table of Contents

In This Issue (p.21)
FDM, 3D, AM, FFF, DIY, and VOCs

Philip Weinsier, IJERI Manuscript Editor

When I first heard a colleague talking about additive manufacturing (AM), I had no idea what she meant, even though I was familiar with 3D printing. It never ceases to amaze me how we come up with such descriptors but, sure, additive manufacturing now makes sense in that there are plenty of different thermoplastic materials that can be used in the process. For example: acrylonitrile butadiene styrene (ABS), polylactic acid, polyethylene terephthalate glycol, polycarbonate, and nylon. Beyond AM, I started hearing about what I could only assume were different processes: fused deposition modeling (FDM) and fused filament fabrication (FFF), which, I discovered, were the same thing, except that the acronym FDM was trademarked.

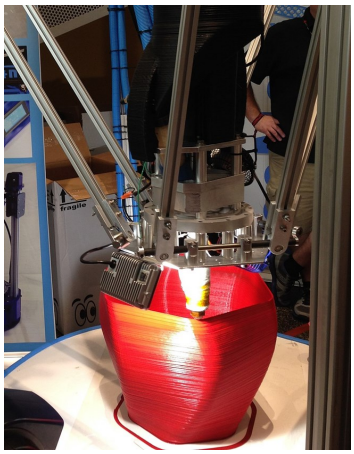

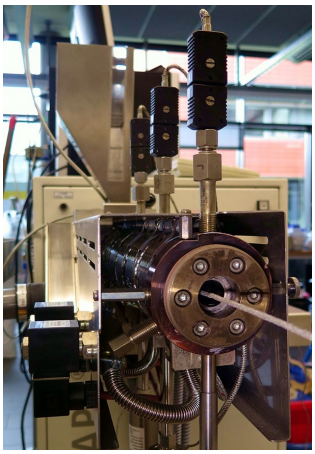

FDM was developed back in 1988 by Stratasys. But their patent on their FDM technology expired in 2009 allowing everyone to use this type of printing. Not long after, of course, industry smelled blood in the water and commercial FFF-based 3D printers got to work in the aerospace, automotive, construction, electronics, energy, sports, textiles, toys, and medical / pharmaceutical fields. By this time, amateurs and institutions were having a field day with DIY projects and open-source 3D printer designs. At its core, 3D printing technology involves the use of a continuous filament of thermoplastic material, fed from a spool through a heated printer extruder head, which melts the material and deposits it layer by layer to create a three-dimensional object. FDM printers are versatile, capable of printing with a wide range of materials, and are user-friendly. Still, their layer-by-layer deposition process can result in visible layer lines and a rough finish as well as structural support parts requiring removal at the end of the printing process.

For this process, users must consider strength, temperature resistance, and other properties, as well as the fact that the different materials come with different advantages and disadvantages. FDM printers and materials are relatively inexpensive, though this hasn't always been the case. 3D printers that once cost $20,000 now can be purchased for less than $1000. Since 2017, several companies are selling parts for users to build their own "RepRap" designs, which can be built for as little as $100. But lest you think that AM is without its risks, filament printers are dangerous to our health and are a major source of volatile organic compounds (VOCs), which are substances that easily dissolve in the air. One study measured over 400 different types of VOCs. 3D printers also emit particulate matter, made up of particles that remain suspended in the air for a long period of time, and ultrafine particles in the 1-100 nanometer range. Such particles are small enough to lodge deep in the respiratory system and be difficult for the body to get rid of.

In our featured article (p.21), the authors examined the tensile properties of ABS components manufactured via FDM. Test specimens were printed using systematically varied combinations of extrusion temperature, layer thickness, and infill density. The resulting tensile data were then used to train several regression models. Among the approaches examined, gradient boosting, support vector regression, and polynomial regression proved to be the most dependable, each accounting for more than 86% of the variation in measured strength. These trained models were then paired with evolutionary optimization methods to search for printing conditions that would yield higher-performing parts. Multiple optimizers converged on parameter regions associated with predicted tensile strengths in the upper 30-megapascal range. From this study, the authors confirmed that pairing machine learning with evolutionary search methods provides an efficient approach to enhancing the tensile performance of ABS components produced by FDM.

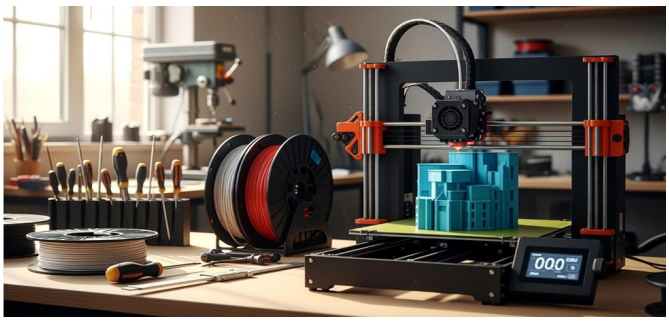

Editorial Review Board Members

Advancing Industry 4.0: Multimodal Sensor Fusion for AI-Based Fault Detection in 3D Printing

Muhammad Fasih Waheed, Florida A&M University; Shonda Bernadin, Florida A&M University; Ali Hassan, Florida A&M University

Abstract

Additive manufacturing, particularly fused deposition modeling, is transforming modern production by enabling rapid prototyping and complex part fabrication. However, its layer-by-layer process remains vulnerable to faults such as nozzle clogging, filament runout, and layer misalignment, which compromise print quality and reliability. Traditional inspection methods are costly, time-intensive, and often limited to post-process analysis, making them unsuitable for real-time intervention. In this current study, the authors developed a novel, low-cost, and portable fault-detection system that leverages multimodal sensor fusion and artificial intelligence for real-time monitoring in FDM-based 3D printing.

The system integrates acoustic, vibration, and thermal sensing into a non-intrusive architecture, capturing complementary data streams that reflect both mechanical and process-related anomalies. Acoustic and thermal sensors operate in a fully contactless manner, while the vibration sensor requires minimal attachment such that it will not interfere with printer hardware, thereby preserving portability and ease of deployment. The multimodal signals are processed into spectrograms and time-frequency features, which are classified using convolutional neural networks for intelligent fault detection. The proposed system advances Industry 4.0 objectives by offering an affordable, scalable, and practical monitoring solution that improves fault-detection accuracy, reduces waste, and supports sustainable, adaptive manufacturing.

Introduction

Additive manufacturing (AM), driven by advancements in digital design and automation, is increasingly revolutionizing the production landscape by enabling rapid prototyping, personalized fabrication, and material-efficient processes. Among the various AM modalities, fused deposition modeling (FDM) holds a prominent position, due to its cost-effectiveness, material flexibility, and widespread accessibility in both industrial and research contexts. Despite these advantages, FDM processes remain vulnerable to a spectrum of faults, ranging from nozzle clogging and filament runout to layer shifting and misalignment, which compromise geometrical fidelity, mechanical properties, and functional integrity of manufactured parts (Sampedro, Rachmawati, Kim & Lee, 2022; Deokar, Kumar & Singh, 2025).

The complex interplay of thermal, mechanical, and dynamic factors during layer-wise deposition introduces numerous opportunities for process instability. For instance, variations in extrusion temperature, inaccuracies in movement axes, and inconsistent filament flow can lead to surface defects, dimensional errors, and even print failure. Causality-guided models and multi-parameter approaches have shown practical value for improving accuracy in fault diagnosis models deployed for FDM, indicating that both material and hardware factors must be inclusively considered. Moreover, faults such as warped layers often arise, due to improper cooling rates or uneven thermal distribution, making traditional post-process analysis increasingly impractical for high-yield operations (Deokar et al., 2025).

Historically, quality assurance in FDM relied on post-production inspection techniques such as surface profilometry, optical metrology, and destructive mechanical testing. While effective for evaluating final parts, these methods are inherently reactive, expensive, and labor-intensive, and do not provide the intervention needed for real-time process optimization. The emergence of sensor-based process monitoring systems represents a paradigm shift. Early approaches deployed single-mode sensors such as accelerometers or acoustic emission microphones to monitor vibrations, temperature fluctuations, and mechanical anomalies. However, single-modal sensing often struggles to robustly generalize fault detection across diverse machines, materials, and operational contexts (Petrich, Snow, Corbin & Reutzel, 2021).

Recent advancements have shifted toward multimodal sensor fusion frameworks, which combine heterogeneous data streams for comprehensive characterization of AM processes. Integrating acoustic, vibration, thermal, and even image-based data has been shown to improve anomaly detection and localization, outperforming single-modality systems in accuracy and adaptability. For example, Sampedro et al. (2022) demonstrated data-driven methodologies using thermocouples, infrared thermometers, and accelerometers to extract time-frequency features for predictive quality monitoring in FDM, while Kousiatza and Karalekas (2016) deployed fiber Bragg grating sensors for spatial temperature and strain mapping. Digital twin systems have further enhanced real-time process monitoring, anomaly detection, and autonomous control; cost-effective digital-twin architectures have demonstrated reliable interventions for quality assurance at scale (Shomenov, Ali, Jyeniskhan, Al-Ashaab & Shehab, 2025).

Artificial intelligence, particularly machine learning and deep learning algorithms, now plays a central role in sensor-based monitoring for AM. Convolutional neural networks (CNNs), SVMs, and deep adversarial learning models have been applied to spectrogram and time-frequency representations of multimodal sensor signals, yielding superior fault discrimination and process diagnostics. Kadam, Kumar, Bongale, Wazarkar, Kamat, and Patil (2021) achieved maximum accuracy in fault diagnosis by integrating SVM with pre-trained AlexNet models for layer-wise defect detection, a strategy effective both in offline training and online implementation (Tan, Huang, Liu, Li & Wu, 2023). Despite promising results, several key limitations persist.

Many deployed systems remain non-portable, intrusive, or cost-prohibitive, and struggle to generalize across different printer architectures and materials. Moreover, few systems robustly support closed-loop control for real-time intervention and process optimization. Addressing these gaps is critical to advancing scalable, adaptive, and intelligent manufacturing (Behseresht, Love, Valdez Pastrana & Park, 2024). In this context, the authors of this current study introduce a novel, portable, and low-cost multimodal sensor fusion system for real-time fault detection in FDM processes. The system integrates acoustic, vibration, and thermal sensing in a combination of contactless and minimally intrusive configurations, enabling seamless deployment across heterogeneous printer environments without hardware modification. Unlike traditional monitoring systems that rely on expensive instrumentation or are restricted to specific platforms, this approach emphasizes accessibility, scalability, and adaptability.

AI-driven classification of spectrogram and time-frequency features ensures robust anomaly detection and real-time process feedback, addressing common faults such as nozzle clogging, filament runout, and layer misalignment. By leveraging multimodal inputs, the system compensates for the limitations of individual sensors, achieving higher resilience to environmental noise and variability in operating conditions. Beyond technical improvements, the proposed framework directly supports Industry 4.0 objectives by advancing sustainable, automated, and data-driven manufacturing. It contributes to reducing material waste, lowering energy consumption, and improving production efficiency, thereby promoting wider adoption of additive manufacturing in industrial, research, and educational settings (Chen, Yao, Feng, Chew & Moon, 2023).

To address these challenges, the objective of this research study was to design and validate a portable, low-cost, and minimally intrusive fault-detection framework for FDM-based 3D printing using multimodal sensor fusion. Specifically, the goals were to: (1) develop an integrated sensing architecture to combine acoustic, vibration, and thermal data for comprehensive process monitoring; (2) transform multimodal signals into time-frequency representations suitable for AI-based analysis; and, (3) implement and assess convolutional neural network models for real-time classification of common FDM faults. Through these goals, the authors sought to advance accessible, scalable, and intelligent quality-assurance solutions aligned with Industry 4.0 manufacturing environments.

Background

Fused deposition modeling (FDM) presents a complex thermo-mechanical environment in which subtle variations in heat transfer, polymer flow, and toolpath execution influence part quality. In the Introduction section above, the authors outlines general challenges and common faults; the deeper technical mechanisms underlying these issues, however, warrant further examination. FDM stability depends strongly on the transient thermal field around the nozzle and build surface, the viscoelastic behavior of semi-molten filament during deposition, and the synchronized operation of motion subsystems. Studies in process physics have shown that small deviations in these domains propagate through subsequent layers, amplifying geometric error, interlayer weakness, and surface discontinuities (Ramírez, Márquez & Papaelias, 2023). Understanding these mechanisms has driven the progression from simple monitoring strategies to sophisticated, sensor-rich diagnostic frameworks.

Traditional approaches to ensuring print quality, such as CT scans, tensile testing, and surface profilometry, have primarily served to verify final part performance rather than monitor the evolving state of the print. Their value lies in precision and detail, but they do not illuminate transient process signatures such as thermal drift, extrusion instability, or resonance events occurring during printing (Fu, Downey, Yuan, Pratt & Balogun, 2021). As production requirements have shifted toward higher throughput and reduced scrap, this gap between process and product analysis has motivated research into proactive, process-embedded measurement techniques.

In response to the limitations of isolated measurements, the field has recently gravitated toward data-centric monitoring and multimodal sensor fusion as a more comprehensive solution. By integrating complementary data streams, such as acoustic emissions, vibration signatures, and thermal readings, researchers have demonstrated improved fault classification accuracy and more reliable characterization of printing states compared to single-modality systems (Kumar, Kolekar, Patil, Bongale, Kotecha, Zaguia & Prakash, 2022). Furthermore, combining these sensor frameworks with modern artificial intelligence (AI) techniques, specifically convolutional neural networks (CNNs), allows researchers to leverage time-frequency features such as spectrograms to achieve robust, automated anomaly detection aligned with the goals of Industry 4.0 for intelligent, connected manufacturing.

Methodology

The proposed fault-detection framework was developed as a portable, low-cost, and adaptable solution for FDM-based 3D printers, with two scalable configurations designed to balance simplicity, accuracy, and deployment flexibility. The first, referred to as the Acoustic Baseline System, employed only airborne sound sensing to demonstrate feasibility. The second, the Hybrid Fusion System, expanded coverage by combining acoustic, vibration, and thermal modalities for robust multimodal monitoring. The Acoustic Baseline System consisted of two condenser microphones arranged as a stereo pair, placed 10 cm apart near the printhead to provide directional sensitivity and reduce environmental noise. The microphones interfaced with a USB sound card connected to a personal computer or a single-board computer, such as a Raspberry Pi, which handled acquisition and signal processing. Data collection was implemented through Python-based libraries such as PyAudio and SoundDevice, allowing dual-channel acquisition in real time.

Preprocessing steps included bandpass filtering to isolate the relevant frequency band (100-1000 Hz) and normalization to standardize signal intensity across recordings. The filtered audio was then transformed into spectrograms using short-time Fourier transform (STFT) or Mel-frequency representations that served as inputs to a convolutional neural network (CNN). The CNN, implemented through the Google Teachable Machine platform and exported to TensorFlow, performed automated classification of normal and faulty states. This setup demonstrated that a minimal hardware footprint was sufficient to identify common anomalies, though its scope was inherently restricted to acoustic signatures and its accuracy was influenced by ambient noise conditions.

The Hybrid Fusion System added a triaxial accelerometer (ADXL335) and a thermal camera (FLIR One Pro). The accelerometer was mounted on the extruder carriage or gantry to measure mechanical vibrations associated with hardware issues such as layer shifts, belt wear, or resonance. Vibration data, sampled through an analog-to-digital converter and processed in Python, provided valuable insight into machine stability that acoustic sensing alone cannot reliably capture. The thermal camera was positioned externally with line-of-sight to the extruder region. Thermal data were captured in grayscale frames at low frame rates sufficient to detect anomalies such as nozzle overheating, cold extrusion zones, and uneven thermal drift across long builds. These thermal patterns could be analyzed independently for anomaly detection or fused into the CNN pipeline alongside acoustic and vibration data to improve classification performance. By combining these three sensing modalities, the Hybrid Fusion System produced a richer representation of the printing process and significantly improved resilience against environmental noise, sensor placement variability, and machine-to-machine differences.

The acoustic channel provided non-intrusive monitoring, the accelerometer added direct mechanical diagnostics with minimal attachment, and the thermal camera captured thermal anomalies without interfering with the print. Multimodal fusion of time-frequency features enhanced fault-detection robustness compared to unimodal systems, addressing limitations in portability and generalizability reported in previous studies. To evaluate the strengths and limitations of each individual sensing modality, a structured comparison was performed across eight common FDM fault types. No single sensor demonstrated consistently high sensitivity across all fault categories. Acoustic sensing performed well for extrusion-related anomalies such as material runout and nozzle clogs, but it was less reliable for mechanically induced faults such as belt slip or layer shifts. The accelerometer exceled at detecting mechanical failures but provided little insight into thermal irregularities.

Thermal imaging, in contrast, identified hot-end drift or cooling faults but contributed minimally to vibration-driven failures. This variability across modalities highlights the limitations of relying on a single sensor and directly motivated the need for a multimodal fusion strategy. The fusion approach leveraged the complementary strengths of all three sensors, thereby improving reliability, expanding fault coverage, and enabling robust detection even under variable environmental or machine conditions. The comparison between both systems highlights the trade-off between simplicity and accuracy. The Acoustic Baseline System offers a simple and cost-effective entry point for fault detection that can be rapidly deployed across any FDM printer. However, it is limited to acoustic anomalies and sensitive to environmental interference. In contrast, the Hybrid Fusion System increases hardware complexity and cost but achieves more reliable classification by leveraging multimodal data streams. Table 1 shows a side-by-side summary of the two configurations presented.

Table 1. Comparison of the Acoustic Baseline and Hybrid Fusion systems.

Feature	Acoustic Baseline System	Hybrid Fusion System
Sensors	Two condenser microphones (stereo)	Stereo microphones + triaxial accelerometer + thermal camera
Hardware	USB sound card, PC or Raspberry Pi	Same + accelerometer with ADC + thermal camera
Software	Python (PyAudio, STFT, CNN)	Python (STFT, vibration FFT, thermal image processing, CNN)
Advantages	Simple, low-cost, rapid deployment	High accuracy, robustness, multimodal sensing
Limitations	Acoustic-only; noise-sensitive	Higher cost and complexity

Figure 1 illustrates the comparative fault-detection capability using multimodal sensor data. Figure 2 shows a system flow diagram of the proposed fault-detection framework for a hybrid fusion system. Input variables were collected from three sensing modalities: acoustic signals, accelerometer data, and thermal imaging. Acoustic and vibration signals were transformed into time-frequency representations using fast Fourier transform (FFT), while thermal data were provided as grayscale frames. These processed inputs were passed into a CNN that performed feature extraction, pattern recognition, and fault classification. The CNN was trained on spectrograms and images derived from both normal and faulty printing conditions, allowing it to generalize across multiple fault types. The model produced probability outputs for each class, and fault conditions were flagged when the probability exceeded a defined threshold (e.g., 80%). This framework enables real-time, AI-based monitoring of FDM printing processes and supports early intervention to reduce material waste and downtime.

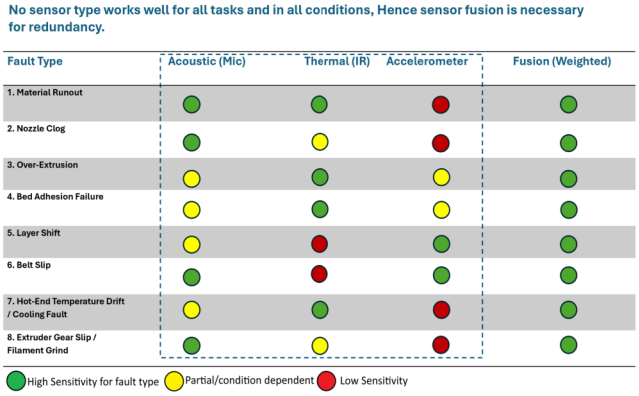

Figure 1. Comparative fault detection capability across multimodal sensors in FDM printing.

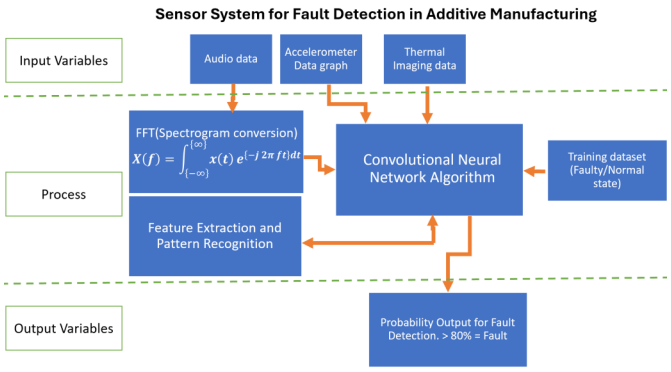

Figure 2. System flow diagram for a hybrid fusion system.

Figure 3 shows two condenser microphones, highlighted with red arrows, which were placed 10 cm apart near the extruder to capture stereo acoustic signals for fault detection. This configuration enabled directional sensitivity by exploiting amplitude differences between the two channels, while also reducing the influence of background noise.

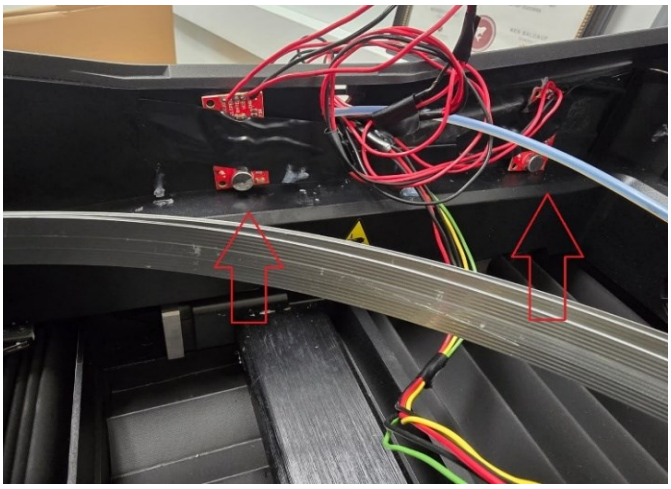

Figure 3. Microphones installed on the FDM machine.

The prototype device, discussed later, had the microphones built in and, for experimentation purposes, were installed on the printer. Figure 4 shows the microphones connected to a sound card and, subsequently, to a Raspberry Pi or personal computer for real-time acquisition. By converting raw audio signals into these representations, the monitoring system was able to extract discriminative features that served as inputs for the CNN classifier. This combination of FFT-based spectral analysis and spectrogram visualization formed the basis of robust acoustic fault detection in the proposed framework.

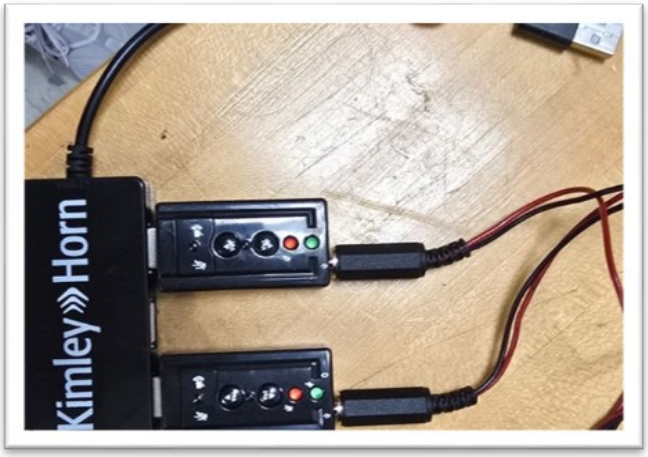

Figure 4. USB sound card for dual-channel recording.

The dual-configuration monitoring system incorporated stereo microphones, a triaxial accelerometer, and a compact thermal camera. Strategic placement of these sensors ensured accurate signal capture, fault detection, and process localization. Two identical condenser microphones were connected to a stereo sound card, arranged as described earlier. This setting enabled directional fault localization by comparing amplitude differences between channels, allowing detection of events such as filament slips or stepper motor skips.

For vibration monitoring, an ADXL335 analog triaxial accelerometer was rigidly attached to the extruder carriage. This placement maximized sensitivity to vibrations generated by belts, guide rails, and stepper motors. The accelerometer signals were routed through an Arduino interface, enabling detection of faults such as backlash, loose belts, or resonance artifacts. Thermal monitoring was achieved using a compact USB-based thermal camera (FLIR Pro), mounted externally with an unobstructed view of the nozzle. Positioned 15-30 cm away, the camera was fixed on a frame to provide consistent alignment. The thermal data allowed detection of cold nozzles, overheating zones, and uneven extrusion temperatures, supporting real-time inference of clogs or flow irregularities. Table 2 shows a summary of sensor placement and purpose.

Table 2. Summary of sensor placement and purpose.

Sensor	Placement	Purpose	Notes
Dual Mics	10 cm apart, facing extruder	Acoustic fault localization via amplitude difference	Avoid fan airflow and frame echoes
ADXL335	On printhead/ gantry	Detects fine mechanical vibrations	Requires secure attachment
Thermal Camera	Outside printer, facing extruder	Detects heating faults, thermal drift	Avoid obstruction; calibrate ambient

A computer system served as the primary data collection and processing device. The system handled acquisition from all sensor channels, performed preprocessing such as filtering and spectrogram generation, and executed CNN-based fault classification in real time. Figures 5 and 6 show the PCB for the Raspberry Pi-based portable system that was developed.

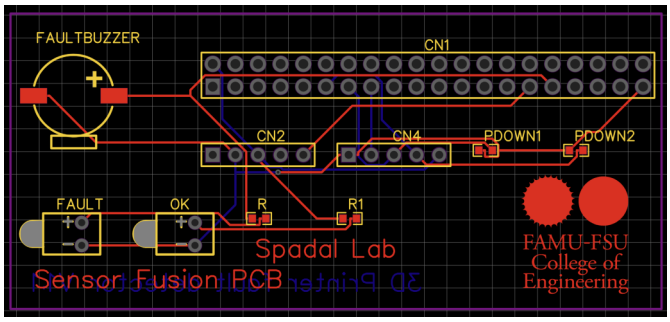

Figure 5. PCB layout of sensor fusion.

Figure 7 shows a schematic diagram for the interface between both the audio sensor and the triaxial accelerometer, with input signals routed through the Raspberry Pi header for real-time processing. The Raspberry Pi performed signal preprocessing and fault classification, while the PCB provided immediate user feedback through a fault-indication LED and buzzer whenever an anomaly was detected. Although the buzzer/LED combination served as a rapid hardware-level alert, the type and classification of the fault were displayed on the Raspberry Pi's graphical user interface (GUI), ensuring both quick detection and detailed reporting. This integrated design enabled seamless multimodal data acquisition and real-time fault indication within a compact, low-cost framework suitable for deployment on FDM 3D printers.

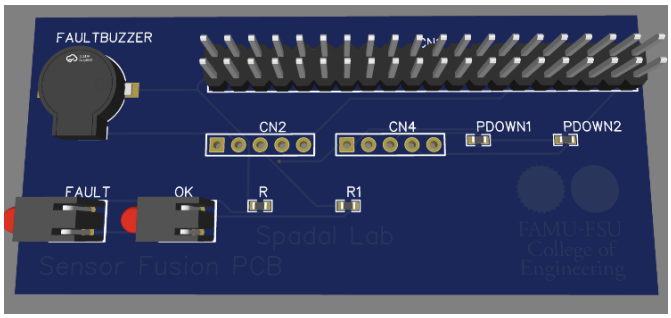

Figure 6. 3D diagram of PCB.

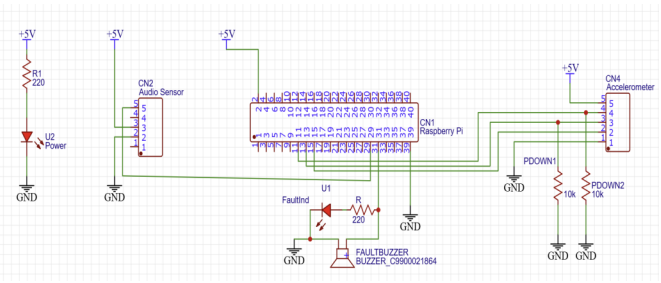

Figure 7. Schematic diagram of PCB.

The raw acoustic and vibration signals acquired from the sensors were first passed through a bandpass filter to isolate the frequency range most relevant to fault detection. Figure 8 shows a 100-1000 Hz window that was selected for the audio channel, as this range effectively captured extrusion-related noise while reducing interference from background sources such as fans or ambient environmental sounds. Similarly, vibration signals were filtered to emphasize machine-induced oscillations and suppress unrelated high-frequency noise.

Following filtering, the processed signal files were used as inputs to the Google Teachable Machine platform, which automatically converted the time-domain signals into spectrograms. These spectrograms represented the energy distribution of the signals across both time and frequency, providing a richer feature space compared to raw waveforms. Once generated, the spectrograms were normalized and resized to maintain uniform dimensions suitable for CNN processing. The CNN extracted relevant patterns associated with normal and faulty conditions, enabling robust classification of nozzle clogging, filament runout, and other print anomalies.

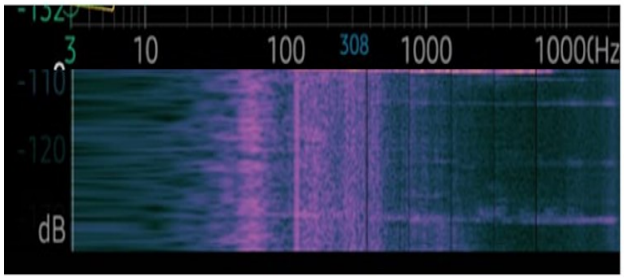

(a) Baseline noise.

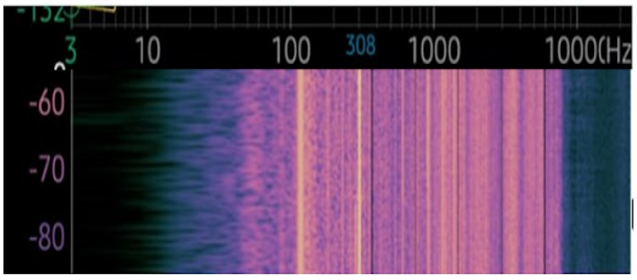

(b) Printer operation sound.

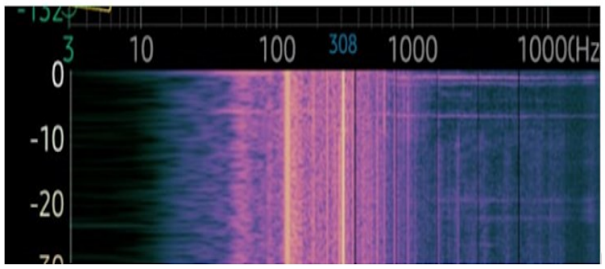

(c) Filtered Sound.

Figure 8. Audio Spectrogram before and after filtering.

Experimental Setup

The experimental framework combined consumer-grade and research-oriented tools to implement and validate the proposed multimodal fault-detection system. A Makerbot Method X FDM printer was used along with a Windows operating system laptop that served as the primary data collection and processing device. Acoustic signals were recorded using a sound card connected to the stereo microphone array, with data acquired and stored for subsequent analysis. Signal preprocessing was performed in MATLAB, where a bandpass filter (100-1000 Hz) was applied to isolate extrusion-related acoustic features and suppress irrelevant noise. The filtered audio files were then imported into Google Teachable Machine, accessed through the Chrome browser, which converted them into spectrograms and used them as inputs for CNN training and inference.

Thermal data were collected using a FLIR One Pro thermal camera paired with an Android smartphone. The thermal behavior of the 3D printer, particularly nozzle heating and extrusion zones, was screen-recorded during operation. These thermal recordings were segmented into representative frames and uploaded into Teachable Machine's image-classification module, where they were processed by a CNN for anomaly detection. For vibration monitoring, an ADXL335 triaxial accelerometer was connected to an Arduino Uno, providing real-time acceleration data along the X, Y, and Z axes. The signals were visualized using the Arduino IDE's serial plotter, and the resulting vibration graphs were screen-recorded. These recordings were then converted into image datasets and uploaded to Teachable Machine, where they were used for CNN-based classification of mechanical anomalies. To simplify the proof-of-concept phase, the experiments focused only on extruder-related faults and material runout conditions. These scenarios were selected because they represent common failure modes in FDM printing and provide clear signatures across acoustic, vibration, and thermal sensing modalities. By limiting the initial tests to these conditions, the system could be validated in a controlled manner, while simultaneously demonstrating its potential for broader fault detection in future studies.

Results

The training of the CNN model on filtered audio files demonstrated rapid convergence, as shown in the accuracy and loss curves. Figure 9 shows that classification accuracy increased sharply within the first 10 epochs and stabilizing thereafter. Training accuracy approached near-perfect levels, while validation (test) accuracy plateaued around 0.90, indicating reliable generalization to unseen data. The corresponding loss curves further support this trend. Both training and test losses decreased significantly during the early epochs, with training loss dropping close to zero and validation loss stabilizing around 0.2 after approximately 15 epochs. This reflects effective feature learning without significant evidence of overfitting, as the validation loss maintained a downward trend and did not diverge from the training loss. Figure 10 shows how the trained audio-based CNN model demonstrated strong capability in distinguishing extrusion faults, as indicated by its detection of the extruder operating without material at 100% accuracy.

During repeated testing, the model consistently maintained a high accuracy level, typically ranging between 90% and 100%. Minor fluctuations were observed, which could be attributed to environmental noise or subtle variations in the acoustic profile across trials. While the audio-only system provided a solid baseline for fault detection, its sensitivity to external interference highlights the need for enhanced robustness. This motivated the incorporation of multimodal sensor fusion, where complementary data from vibration and thermal sensors could reinforce classification reliability and reduce the risk of misclassification.

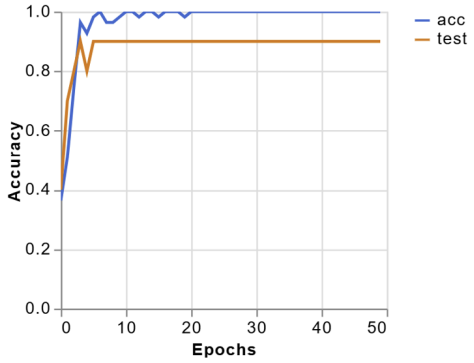

(a) Accuracy per epoch.

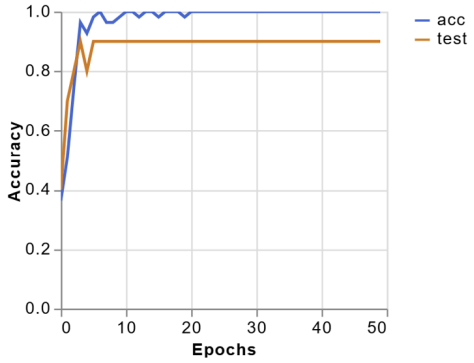

(b) Loss per epoch.

Figure 9. Training and validation accuracy and loss per epoch for audio-based CNN classification.

Figure 10 further shows that the CNN, trained on acoustic features, was able to identify the extrusion-with-material condition reliably, though the accuracy varied between 85% and 95% in repeated tests. This variation was attributed to ambient noise and the similarity of acoustic signatures with other machine states. These results emphasized the strength of the audio-based approach, while also highlighting the potential improvements achievable through multimodal sensor fusion. Thermal imaging provided a clear and interpretable signature of extrusion states. Figure 11 shows that, during normal operation, the nozzle displayed a stable thermal profile with consistent heating at the extrusion zone, confirming steady material flow. Figure 12, in contrast, shows that the clogged or material runout condition was characterized by localized overheating around the nozzle and a lack of downstream thermal continuity, reflecting the absence of deposited filament. These differences make thermal data highly effective for distinguishing extrusion faults in real time. However, thermal imaging alone may be influenced by ambient temperature variations, camera angle, or resolution limitations. As such, while thermal cues provide strong evidence of extrusion anomalies, integrating them with acoustic and vibration data through multimodal sensor fusion can substantially enhance fault-detection accuracy and robustness across diverse printing environments.

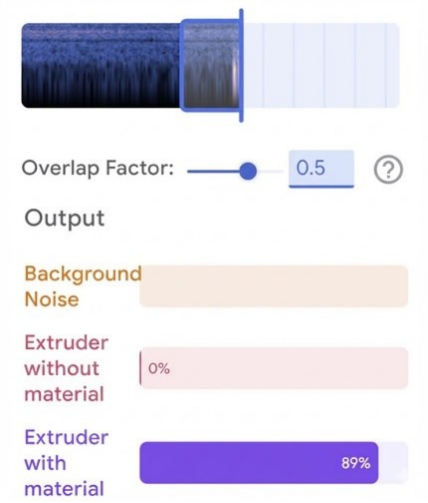

(a) Extruder with material.

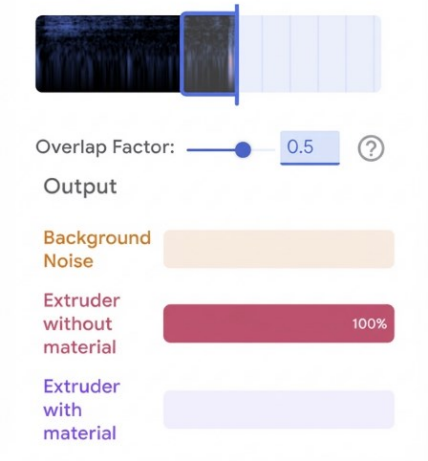

(b) Extruder without material.

Figure 10. Real-time classification output shows the extruder operating with and without material. Note the classification accuracies are 89% and 100%, respectively.

Figure 13 shows that, for further processing, thermal recordings from the FLIR One Pro were segmented into representative frames and uploaded to Teachable Machine for model training and testing. Two primary classes were created: extrusion with material and extrusion without material, as illustrated in the dataset samples. The platform converted these thermal images into feature-rich representations suitable for CNN processing. During testing, the model was able to clearly differentiate between the two states, achieving 100-percent classification accuracy under controlled conditions. Figure 14 shows the strong contrast in heat distribution patterns between normal extrusion and material runout that provided reliable cues for fault detection, demonstrating that thermal imaging is a highly effective modality for identifying extrusion-related anomalies in real time.

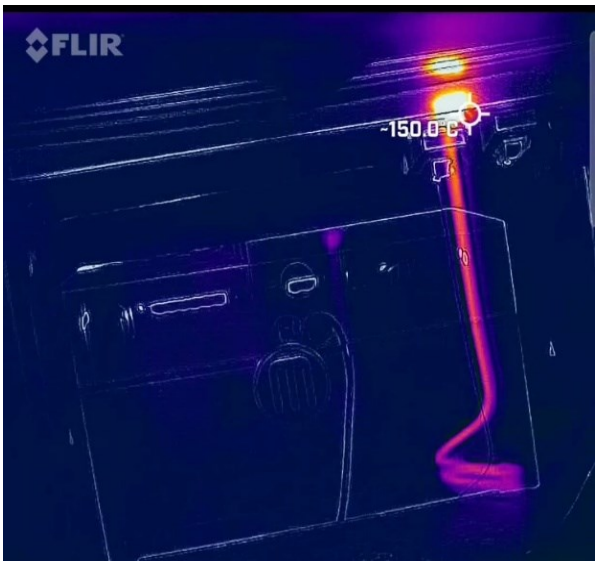

Figure 11. Normal extrusion. Note that the material coming out from the extruder is warmer than surroundings.

Figure 12. Material run-out condition. Note that the extruder is warm but there is no extrusion of material—old material is losing heat.

The accelerometer channel did not yield significant results during the initial tests, as the extrusion process involved very little movement in each axis. This limited vibration activity made it difficult for the sensor to capture discriminative features for fault detection under the chosen test conditions. However, the accelerometer is expected to be more effective in future experiments involving dynamic carriage movements, belt-driven faults, or mechanical instabilities, where vibration signatures are more pronounced. Incorporating such scenarios will allow the vibration modality to contribute meaningfully to the multimodal fusion framework.

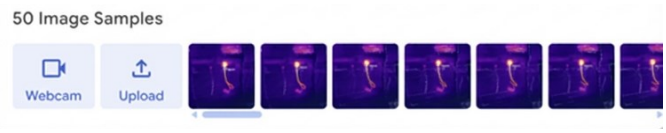

a) Thermal imaging samples with material.

b) Thermal imaging samples without material.

Figure 13. Thermal dataset samples uploaded to Teachable Machine for model training.

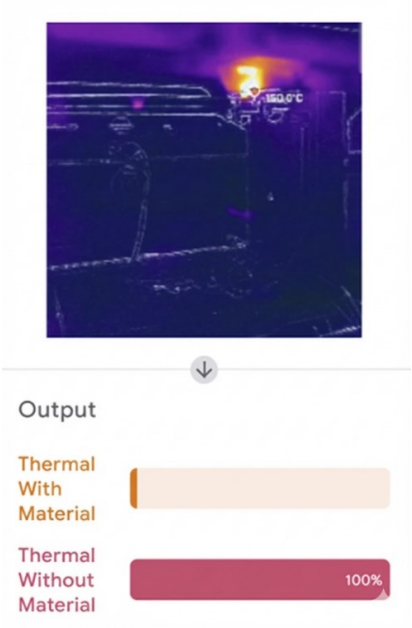

Figure 14. Real-time classification output from thermal imaging shows the extruder without material detected with 100% accuracy. The model successfully identified the absence of extrusion flow, based on distinct thermal patterns around the nozzle.

Conclusions

In this study, the authors introduced and validated a portable, low-cost, and AI-driven fault-detection system for fused deposition modeling (FDM) that leveraged multimodal sensor fusion. By combining acoustic, vibration, and thermal sensing in complementary configurations, the proposed framework demonstrated strong potential for overcoming the limitations of single-modality monitoring. Experimental results showed that the acoustic-only system provided a solid baseline for anomaly detection, while the hybrid fusion system significantly improved robustness and classification accuracy by mitigating noise sensitivity and capturing broader process signatures. A quantitative comparison with existing approaches showed that the

proposed multimodal fusion system performed competitively with, and in some cases exceeded, state-of-the-art methods. In prior studies of vibration-only systems, Mishra, Powers, and Kate (2023) reported classification accuracies of approximately 92 percent for detecting nozzle blockage and filament anomalies, while Kumar et al., (2022) looked at multimodal systems integrating acoustic, thermal, and current sensing and found that they typically achieved 90 to 94 percent accuracy, though often requiring specialized data acquisition hardware and intrusive sensor placement.

In comparison, their acoustic-only baseline system achieved 85 to 95 percent class-wise accuracy, depending on ambient noise, while the thermal imaging subsystem reached 100 percent accuracy in distinguishing extrusion versus non-extrusion states under controlled conditions. Although accelerometer data were less informative during static extrusion, the combined multimodal architecture was expected to yield 90 to 95 percent accuracy, while remaining fully portable, non-intrusive, and being relatively low in cost. This quantitative comparison underscores the benefits of multimodal sensing in achieving a strong balance of accuracy, affordability, and ease of deployment.

The CNN-based classification pipeline effectively translated sensor signals into actionable insights, enabling real-time detection of nozzle clogging, filament runout, and extrusion anomalies. Thermal imaging further enhanced interpretability of fault states and vibration sensing, while being less effective in static extrusion tests; it was, nonetheless, expected to contribute meaningfully under dynamic machine conditions. Together, these modalities establish a scalable monitoring solution that is minimally intrusive, adaptable across heterogeneous platforms, and aligned with Industry 4.0 principles. Beyond technical contributions, the system directly supports sustainability goals by reducing waste, preventing failed builds, and extending the reliability of additive manufacturing. With further refinement, particularly in integrating vibration features, expanding datasets, and exploring closed-loop control mechanisms, this framework can evolve into a fully autonomous quality assurance system. Ultimately, the presented approach advances the vision of intelligent, data-driven manufacturing systems capable of supporting industrial, research, and educational applications at scale.

References

Behseresht, S., Love, A., Valdez Pastrana, O. A., & Park, Y. H. (2024). Enhancing fused deposition modeling precision with serial communication-driven closed-loop control and image analysis for fault diagnosis-correction. *Materials (Basel), 17*(7), 1459. https://doi.org/10.3390/ma17071459

Chen, L., Yao, X., Feng, W., Chew, Y., & Moon, S. K. (2023). Multimodal sensor fusion for real-time location -dependent defect detection in laser-directed energy deposition. *arXiv preprint arXiv:2305.13596.* https://arxiv.org/abs/2305.13596

Deokar, S., Kumar, N., & Singh, R. P. (2025). A comprehensive review on smart manufacturing using machine learning applicable to fused deposition modeling. *Results in Engineering, 26,* 104941. https://doi.org/10.1016/j.rineng.2025.104941

Fu, Y., Downey, A., Yuan, L., Pratt, A., & Balogun, Y. (2021). In situ monitoring for fused filament fabrication process: A review. *Additive Manufacturing, 38,* 101749. https://doi.org/10.1016/j.addma.2020.101749

Kadam, V., Kumar, S., Bongale, A., Wazarkar, S., Kamat, P., & Patil, S. (2021). Enhancing surface fault detection using machine learning for 3D printed products. *Applied System Innovation, 4,* 34. https://doi.org/10.3390/asi4020034

Kousiatza, C., & Karalekas, D. (2016). In-situ monitoring of strain and temperature distributions during fused deposition modeling process. *Materials & Design, 97,* 400-406. https://doi.org/10.1016/j.matdes.2016.02.099

Kumar, S., Kolekar, T., Patil, S., Bongale, A., Kotecha, K., Zaguia, A., & Prakash, C. (2022). A low-cost multi-sensor data acquisition system for fault detection in fused deposition modelling. *Sensors, 22,* 517. https://doi.org/10.3390/s22020517

Mishra, R., Powers, W. B., & Kate, K. (2023). Comparative study of vibration signatures of FDM 3D printers. *Progress in Additive Manufacturing, 8*, 205-209. https://doi.org/10.1007/s40964-022-00323-5

Petrich, J., Snow, Z., Corbin, D., & Reutzel, E. W. (2021). Multi-modal sensor fusion with machine learning for data-driven process monitoring for additive manufacturing. *Additive Manufacturing, 48*(B), 102364. https://doi.org/10.1016/j.addma.2021.102364

Ramírez, I. S., Márquez, F. P. G., & Papaelias, M. (2023). Review on additive manufacturing and non-destructive testing. *Journal of Manufacturing Systems, 66,* 260-286. https://doi.org/10.1016/j.jmsy.2022.12.005

Sampedro, G. A. R., Rachmawati, S. M., Kim, D. S., & Lee, J. M. (2022). Exploring machine learning-based fault monitoring for polymer-based additive manufacturing: Challenges and opportunities. *Sensors (Basel), 22*(23), 9446. https://doi.org/10.3390/s22239446

Shomenov, K., Ali, M. H., Jyeniskhan, N., Al-Ashaab, A., & Shehab, E. (2025). Cost-effective sensor-based digital twin for fused deposition modeling 3D printers. *International Journal of Computer Integrated Manufacturing,* 1-20. https://doi.org/10.1080/0951192X.2025.2504085

Tan, L., Huang, T., Liu, J., Li, Q., & Wu, X. (2023). Deep adversarial learning system for fault diagnosis in fused deposition modeling with imbalanced data. *Computers & Industrial Engineering, 176,* 108887. https://doi.org/10.1016/j.cie.2022.108887

Zhu, X., Kumar, P., & Lee, J. M. (2022). A low-cost multi-sensor data acquisition system for fault detection in fused deposition modelling. *Sensors (Basel), 22*(2), 517. https://doi.org/10.3390/s22020517

Biographies

MUHAMMAD FASIH WAHEED is a PhD candidate in electrical engineering at the FAMU-FSU College of Engineering at Florida A&M University. He received his MS degree in electrical engineering from Florida A&M University and his BE degree in electrical engineering from Hamdard University. His research interests include sensor technologies, artificial intelligence, additive manufacturing (3D printing), and wireless communication systems. He has extensive experience in developing intelligent monitoring frameworks and sensor-driven solutions for real-time fault detection and process optimization. Mr. Waheed may be reached at muhammad1.waheed@famu.edu

SHONDA BERNADIN is a Google Endowed Full Professor in the Department of Electrical and Computer Engineering at the FAMU-FSU College of Engineering. Dr. Bernadin received her BS in Electrical Engineering from Florida A&M University, her MS in Electrical and Computer Engineering from University of Florida, and her PhD in Electrical Engineering from Florida State University. Her research interests include speech and image processing, data analysis, natural language processing, artificial intelligence, acoustic sensor integration, and semiconductor manufacturing and technologies. She is also very active in engineering education and outreach programs that seek to broaden engineering talent in the STEM workforce. Dr. Bernadin may be reached at bernadin@eng.famu.fsu.edu

ALI HASSAN is a PhD student in electrical engineering in the FAMU-FSU College of Engineering, Department of Electrical and Computer Engineering. He earned his Bachelor of Science in Electrical Engineering degree from the Information Technology University, Lahore, Punjab. His current research focuses on using artificial intelligence for signal processing. Mr. Hassan may be reached at ali1.hassan@famu.edu

Generating a Labeled 3D Box Dataset for Machine Learning to Localize a Box

Faruk Ahmed, University of Memphis; Kevin Berisso, University of Memphis

Abstract

Automatically localizing a box of different sizes using machine learning (ML) requires a dataset to train an ML model. Figure 1 shows SICK's Visionary-T 3D camera (Visionary-T - Archive | SICK, n.d.) that natively offers only a binary indication of whether an object matches a predefined box size, leaving position, orientation, and dimensional estimation unaddressed. To bridge this gap, a comprehensive workflow was devised in this current study to capture and annotate point-cloud data for boxes of different sizes and aspect ratios. Three hundred scenes were recorded under varying distances and viewpoints then processed by an automatic labeling pipeline that inferred each box's six-degree-of-freedom pose and edge lengths. The automated procedure yielded valid annotations for roughly 25 % of the samples, producing an initial, openly available dataset that could be progressively refined through human verification. Once corrected, the dataset enabled the training of ML models capable of simultaneously estimating position, orientation, and size, thereby facilitating accurate grasp planning and collision-free manipulation for industrial robotic hands. This resource can accelerate research on 3D perception, lower the entry barrier for experimentation, and pave the way for fully data-driven box-handling solutions in automated logistics.

Figure 1. Visionary-T 3D camera from SICK.

Problem Statement

The objective of this study was to accurately predict the position, orientation, and size of a box within a 3D scene—a task that is inherently complex. A point cloud image is necessary for this type of prediction, because the point cloud keeps the depth information along with 2D information. The point cloud image of Figure 2 illustrates a typical scenario in which the mesh represents the overall area of a box that is located on the floor. In real-world settings, the presence of other objects further complicates the challenge, as the system must first identify which object in the scene is the box. Once the box is correctly detected, the next step is to estimate its spatial position, orientation, and dimension.

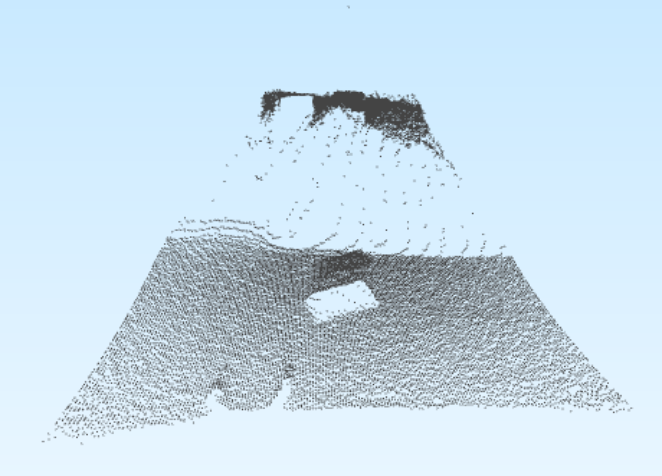

Figure 2. A sample point cloud showing the mesh.

Solution Strategy

For the task of box localization, the development of a suitable dataset requires systematic collection of point cloud data from boxes of varying sizes. The experimental design involves positioning boxes at different distances and orientations, with their physical dimensions measured in advance to ensure accurate ground truth. The acquired point cloud data undergoes initial automatic annotation, followed by manual refinement using labelCloud software to correct errors and ensure high-quality labels (Sager, Zschech & Kühl, 2021; Sager, Zschech & Kühl, 2022). All image and point cloud acquisitions in this study were performed on a workstation running Ubuntu 24.04. The data processing pipeline integrated OpenCV and Open3D, along with Python libraries specific to SICK devices, to enable acquisition, visualization, and annotation of the 3D data.

Literature Review

Detecting box-shaped objects in 3D point clouds is critical in computer vision, robotics, autonomous navigation, and industrial automation (Fan, Cao, Liu, Li, Deng, Sun & Peng, 2024; Paigwar, Erkent, Wolf & Laugier, 2019; Sapkota, Roumeliotis, Cheppally, Calero & Karkee, 2025). Unlike 2D detection, the challenges in 3D arise from sparsity, occlusion, noise, and the unstructured nature of point cloud

data (Sha, Gao, Zeng, Li, Li, Zhang & Wang, 2024; Shao, Sun, Tan & Yan, 2023). Early research focused on handcrafted geometric features such as curvature, surface normals, and spin images, combined with classical classifiers like random forests and support vector machines (SVMs) (Rusu, Blodow & Beetz, 2009). For box detection, algorithms such as RANSAC (random sample consensus) and Hough Transform were widely applied to fit geometric primitives (Schnabel, Wahl & Klein, 2007). These approaches, however, are sensitive to noise and demand extensive parameter tuning.

The introduction of deep learning transformed point cloud analysis. Architectures like PointNet and PointNet++ (Qi, Su, Kaichun & Guibas, 2017) process raw points directly, learning both local and global features without the need for voxelization. VoteNet (Qi, Litany, He & Guibas, 2019) extended this to 3D bounding box regression by combining learned features with a Hough voting scheme, enabling accurate estimation of object centers, dimensions, and orientations. Voxelization offers a structured grid representation that supports 3D CNNs, as demonstrated in VoxelNet (Zhou & Tuzel, 2018). While efficient for convolution, voxelization may introduce high memory costs and resolution loss. To address this, hybrid frameworks such as SECOND, PV-RCNN (Shi et al., 2022) and 3DSSD integrate voxel-, point-, and image-based features, achieving state-of-the-art results in LiDAR-based object detection for autonomous systems.

Building on these developments, the authors of this current study proposed a method that focuses specifically on box localization in industrial scenes. Unlike voxel- or hybrid-heavy pipelines that prioritize large-scale outdoor detection, this approach emphasizes accurate bounding box alignment in controlled environments. By combining classical techniques such as RANSAC with tailored normalization and annotation strategies, this current study bridges traditional geometry-driven methods with the annotation efficiency required to generate training datasets for modern deep learning models.

Visionary-T 3D camera

The Visionary-T 3D camera sensor by SICK operates on time-of-flight (ToF) technology, which measures the distance to objects by calculating the time it takes for emitted infrared light to travel to a surface and reflect back to the sensor. The camera projects modulated light pulses into the scene, and a high-speed sensor array captures the reflected signals. By analyzing the phase shift or the travel time of these signals, the device generates a dense depth map or 3D point cloud that represents the spatial structure of the environment. The Visionary-T camera combines depth information with grayscale intensity images, allowing it to provide both geometric and visual data. Its compact design and real-time 3D measurement capabilities make it especially suitable for applications such as object recognition, robotic guidance, and obstacle detection in industrial automation.

In this current study, the goal was to localize boxes traveling on a conveyor belt so that a robot manipulator could be used efficiently. Collecting a comprehensive dataset of boxes can enable solutions to both automatic box identification and the estimation of each box's position, orientation, and size. This motivates the development of a dedicated point cloud box (PCB) database. The Visionary-T 3D camera is a better choice for detecting boxes on a conveyor belt due to its ability to generate dense, grid-aligned 3D point clouds using time-of-flight technology.

Unlike LiDAR, which produces sparse data, or 2D color cameras that lack depth perception, the Visionary-T provides accurate spatial measurements of object dimensions, position, and orientation in real time. This is especially useful in industrial settings where precise detection and tracking of objects are critical. Its compact, solid-state design makes it more robust and cost-effective than many LiDAR systems, and its output is not affected by object color or ambient lighting, unlike 2D cameras. The camera also offers high frame rates and delivers both depth and grayscale images, enabling reliable object identification and fast decision-making. By avoiding the need for complex multi-sensor setups and reducing calibration requirements, the Visionary-T simplifies integration and maintenance, making it an ideal solution for automation tasks involving box detection on moving conveyor systems.

The RANSAC algorithm is particularly suitable for box detection on a conveyor belt using 3D point cloud data due to its robustness, simplicity, and efficiency in fitting geometric models in the presence of noise and outliers. In conveyor belt environments, point clouds collected by a sensor such as the Visionary-T often contain noise, partial occlusions, background clutter, and overlapping objects. RANSAC addresses these challenges by iteratively selecting random subsets of data, fitting geometric models (e.g., planes, cuboids), and evaluating how well the inliers conform. For box detection, it can identify planar surfaces such as the tops and sides of boxes and then reconstruct the overall structure by combining these planes.

A key advantage of this method is that it does not require prior knowledge of object position or exact dimensions, allowing it to adapt to boxes of varying sizes and orientations. On a conveyor belt, the presence of flat surfaces and right angles aligns well with its ability to model planes and axis-aligned shapes. Its relatively low computational demand also enables near real-time processing, which is critical in high-throughput industrial operations. Although end-to-end deep learning models provide advanced capabilities, this geometric fitting approach remains a practical choice in controlled environments, where objects are regular, the scene is structured, and interpretability is important. In such cases, it serves as a strong baseline or complementary technique for 3D box detection, balancing reliability, efficiency, and adaptability.

Point Cloud File Format

There are many file formats that are used to deal with the 3D representation of a scene or point cloud. Point clouds can be stored in various file formats, depending on the source, application, and desired features such as compression, metadata, or color information. Some of the common file formats are noted here. The PLY and PCD files were used in this current study.

- Polygon file format (PLY)
- Point cloud data format (PCD) of the point cloud library (PCL)
- LiDAR data exchange format (LAS/LAZ)
- Plain text with x, y, z coordinates (XYZ)
- Wavefront includes geometry and optionally color/texture (OBJ)
- Leica point cloud format, usually with color and intensity (PTS)
- ASTM format supporting 3D imaging data, often from LiDAR or 3D cameras (E57)

The PLY is a flexible and widely used format originally developed at Stanford University to store 3D models and point clouds. It supports both ASCII and binary encoding and can store not just the 3D coordinates (x, y, z) but also attributes such as color (r, g, b), intensity, normals, and even polygonal faces. After the header, the file contains one line per point, listing values in the order defined in the header.

```
ply
format ascii 1.0
element vertex 1000
property float x
property float y
property float z
property uchar red
property uchar green
property uchar blue
end_header
```

PCD is the native file format of the point cloud library (PCL) and was designed specifically for storing and loading large 3D point cloud datasets. PCD supports ASCII, binary, and compressed binary formats, and allows flexible definition of fields such as x, y, z, r, g, b, normal_x, intensity. Each line after the header represents a point with values corresponding to the listed fields.

```
# .PCD v0.7 – Point Cloud Data file format
VERSION 0.7
FIELDS x y z rgb
SIZE 4 4 4 4
TYPE F F F U
COUNT 1 1 1 1
WIDTH 1000
HEIGHT 1
POINTS 1000
DATA ascii
```

Methodology

Initial point cloud data collection faced two major challenges: identifying boxes within cluttered scenes and efficiently labeling them with 3D bounding boxes. Manual annotation proved impractical for scaling, especially across 300 collected scenes. Depth capture was also inconsistent when the box was directly beneath the camera, requiring repositioning to better reveal the Z-axis. Figure 3 shows an experimental setup.

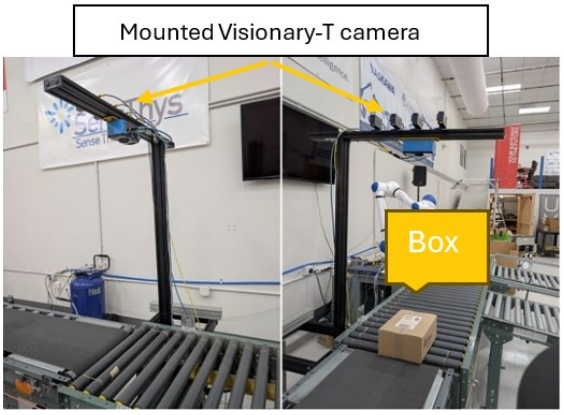

Figure 3. Experimental setup for point cloud collection: the Visionary-T camera is mounted above a conveyor belt transporting boxes. Pictures are shown from two different angles.

To simplify annotation, experiments confirmed that reflective surfaces were not the issue; rather, the camera performed better when objects were placed farther than two feet away. Several annotation tools were tested. While labelCloud offered efficient bounding box labeling, it initially failed to render custom PLY files, due to formatting differences and unusually large coordinate values. In contrast, tools like MeshLab, CloudCompare, and Blender successfully displayed the data but lacked efficient labeling capabilities. The resolution came through coordinate normalization. By adjusting the scale of x, y, and z values to match the range expected by labelCloud, and carefully preserving intensity attributes during processing, the point clouds were finally rendered correctly. With this normalization step, labelCloud became usable for reliable annotation of 3D bounding boxes. The following shows the PLY file that required normalization.

```
ply
format ascii 1.0
comment Exported by SUIT
element vertex 25344
property float32 x
property float32 y
property float32 z
property float32 i
end_header
-1144.647 926.18384 1474.9042 0.0033875029
-1134.5762 928.78485 1464.8997 0.0036011292
-1113.8896 922.6544 1469.5516 0.004180972
```

To apply machine learning for automatic 3D bounding box detection, a properly annotated dataset is required. For this purpose, the collected point cloud data of boxes is annotated programmatically, followed by manual correction of the bounding boxes. Once this process is complete, the dataset becomes suitable for training a machine learning model. Detecting a box in a point cloud involves identifying planar surfaces and estimating a 3D bounding box that encloses them. After performing down sampling and noise removal, clusters of points are extracted, with the assumption that the largest cluster corresponds to the box. Figure 4 shows that, although this step successfully detects a bounding box, it typically aligns only with the visible surface of the box, resulting in inaccurate height estimation.

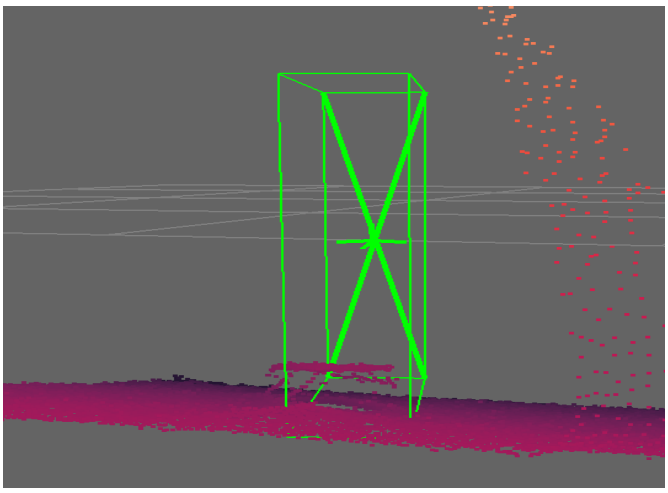

Figure 4. The automatic detection algorithm detects the box but the dimension is much larger than the actual box.

To improve the accuracy, the strategy was adjusted further. Once the surface was identified, nearby points along the Z-axis (height direction) were extracted from the original point cloud, which was limited to the XY extent of the detected surface. A bounding box was then fitted to this combined set of points, resulting in a more accurate approximation of the complete box. Table 1 shows the sizes of the boxes. A statistical technique, principal component analysis (PCA), was used for this task. PCA helps to cluster points belonging to a single box by identifying the principal axes along which the points are most spread out. By computing the eigenvectors and eigenvalues of the covariance matrix of a point cluster, PCA reveals the length, width, and height directions of a box. Figure 5 shows that this is particularly useful for fitting oriented bounding boxes (OBBs) instead of axis-aligned boxes, especially when boxes are placed at arbitrary angles on a conveyor belt.

The authors observed that the bounding box orientation was misaligned, likely due to the use of PCA, which can tilt or skew the box when the point cloud is sparse, noisy, or unevenly distributed. To address this issue, RANSAC was applied for clustering, as it provided greater robustness compared to PCA. Only the points tightly aligned with the surface were used to compute accurate XY bounds. A narrow vertical range along the Z-axis was then defined using the 99th percentile of the height values after which the bounding box was fitted to this clean subset. Figure 6 indicates that the resulting bounding box showed a much closer match to the expected shape and orientation.

Table 1. Sizes of the boxes.

Box	Height (inches)	Width (inches)	Length (inches)
1	3.5	5	14.5
2	7	8.5	11.5
3	7.75	10	11.5
4	5.5	9	11
5	3	5.5	7

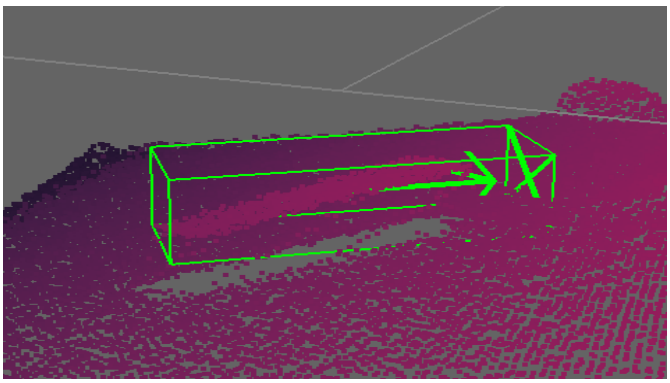

Figure 5. Bounding box detection refined with PCA to approximate actual box size; orientation remains misaligned.

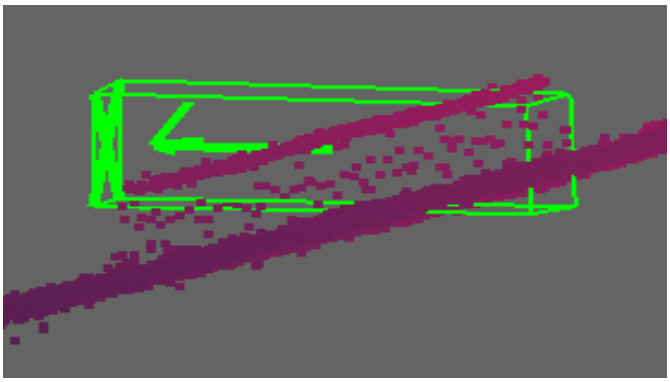

Figure 6. Bounding box detection and orientation improved with RANSAC clustering, yielding a closer match to the expected box shape.

The automatic labeling produced correct bounding boxes in roughly 25% of the cases. While this accuracy is limited, its practical advantage is that in labelCloud the bounding box is already pre-placed. As a result, the annotator does not need to draw a new box from scratch but only refine its position and dimensions to match the actual box, which

significantly reduces the manual correction effort. The software provided with the Visionary-T camera was used to capture point cloud data. Point clouds were collected for five boxes of varying sizes. To preserve size-related information, separate folders were created. The labelCloud is a very efficient and lightweight bounding box labeling software package. It produces centroid [x, y, z], dimensions [length, width, height], and relative rotations as Euler angles in radians from -pi to +pi in yaw, pitch, and roll for each bounding box. There are no units for the dimensions because the original point cloud is normalized. Figure 7 shows the labelCloud interface.

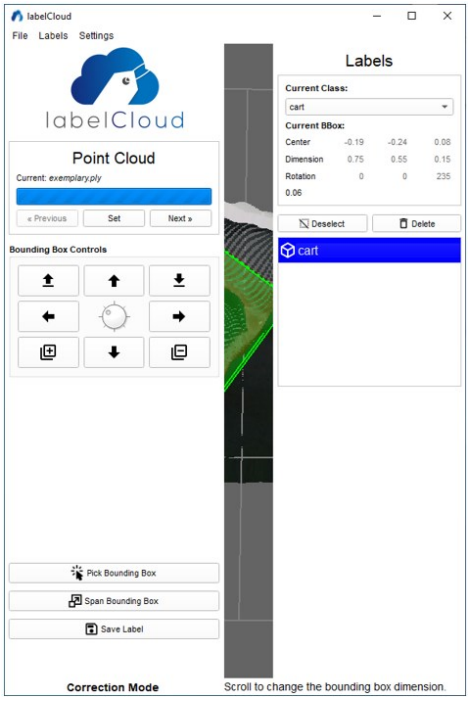

Figure 7. labelCloud annotation software user interface.

The final database contained the point cloud file in PLY or PCD format in a folder with corresponding labels in another folder. Below is a sample label of the point cloud file. Figure 8 shows a simple flow diagram to illustrate the key steps of the workflow.

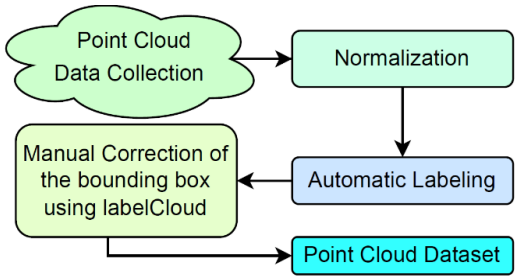

Figure 8. Visual summary of the workflow of the overall process of the point cloud dataset.

Conclusions

In this study, the authors used a Visionary-T 3D camera to capture point clouds of boxes and an initial automatic labeling process was developed for box identification. Since the automatic labeling exhibited imperfections, manual corrections were performed to ensure data integrity. The resulting dataset, entitled the Point Cloud Box (PCB) dataset, established a reliable foundation for training machine learning models aimed at accurate box localization in 3D space. Beyond its role as a research dataset, the PCB dataset has direct implications for industrial automation. Accurate 3D box localization enables robotic arms to identify, grasp, and manipulate packages in warehouses, thereby streamlining logistics and reducing labor costs. Shown here is a sample label of a point cloud file with a box.


```
{
  "folder": "pointclouds_scaled",
  "filename": "Frame2587_scaled.ply",
  "path": "pointclouds_scaled\\Frame2587_scaled.ply",
  "objects": [
    {
      "name": "box",
      "centroid": {
        "x": -0.16449232868591723,
        "y": -0.3035790747445425,
        "z": 0.36742769532991976
      },
      "dimensions": {
        "length": 1.18,
        "width": 0.61,
        "height": 3.05
      },
      "rotations": {
        "x": 0.0,
        "y": 0.0,
        "z": 1.78285556
      }
    }
  ]
}
```


In manufacturing environments, it supports automated assembly lines by allowing robots to detect and position components with precision. In quality control, machine learning models trained on this dataset can identify misplaced or defective items. More broadly, improved box detection enhances supply chain efficiency, inventory tracking, and autonomous navigation in production facilities. With the corrected dataset in place, the next step is to expand its scope by incorporating more diverse scenes and box variations, ultimately training robust machine learning models capable of supporting high-accuracy automation across manufacturing and production systems.

References

Fan, L., Cao, J., Liu, X., Li, X., Deng, L., Sun, H., & Peng, Y. (2024). Voxel self-attention and center-point for 3D object detector. *iScience*, *27*(9), 110759. https://doi.org/10.1016/j.isci.2024.110759

Paigwar, A., Erkent, O., Wolf, C., & Laugier, C. (2019). Attentional PointNet for 3D-Object Detection in Point Clouds. *2019 IEEE/CVF Conference on Computer Vision and Pattern Recognition Workshops (CVPRW)*, 1297-1306. https://doi.org/10.1109/cvprw.2019.00169

Qi, C. R., Litany, O., He, K., & Guibas, L. J. (2019). Deep Hough Voting for 3D Object Detection in Point Clouds. *Proceedings of the IEEE International Conference on Computer Vision*. https://doi.org/10.48550/arXiv.1904.09664

Qi, C. R., Su, H., Kaichun, M., & Guibas, L. J. (2017). PointNet: Deep Learning on Point Sets for 3D Classification and Segmentation. *2017 IEEE Conference on Computer Vision and Pattern Recognition (CVPR)*, 77-85. https://doi.org/10.1109/CVPR.2017.16

Rusu, R. B., Blodow, N., & Beetz, M. (2009). Fast Point Feature Histograms (FPFH) for 3D registration. *2009 IEEE International Conference on Robotics and Automation*, 3212-3217. https://doi.org/10.1109/ROBOT.2009.5152473

Sager, C., Zschech, P., & Kühl, N. (2021). labelCloud: A Lightweight Domain-Independent Labeling Tool for 3D Object Detection in Point Clouds. https://doi.org/10.48550/arXiv.2103.04970

Sager, C., Zschech, P., & Kuhl, N. (2022). labelCloud: A Lightweight Labeling Tool for Domain-Agnostic 3D Object Detection in Point Clouds. *Computer-Aided Design and Applications*, *19*(6), 1191-1206. https://doi.org/10.14733/cadaps.2022.1191-1206

Sapkota, R., Roumeliotis, K. I., Cheppally, R. H., Calero, M. F., & Karkee, M. (2025). A Review of 3D Object Detection with Vision-Language Models (arXiv:2504.18738). arXiv. https://doi.org/10.48550/arXiv.2504.18738

Schnabel, R., Wahl, R., & Klein, R. (2007). Efficient RANSAC for Point-Cloud Shape Detection. *Computer Graphics Forum*, *26*(2), 214-226. https://doi.org/10.1111/j.1467-8659.2007.01016.x

Sha, H., Gao, Q., Zeng, H., Li, K., Li, W., Zhang, X., & Wang, X. (2024). SPBA-Net point cloud object detection with sparse attention and box aligning. *Scientific Reports*, *14*(1), 28420. https://doi.org/10.1038/s41598-024-77097-z

Shao, Y., Sun, Z., Tan, A., & Yan, T. (2023). Efficient three -dimensional point cloud object detection based on improved Complex-YOLO. *Frontiers in Neurorobotics*, *17*. https://doi.org/10.3389/fnbot.2023.1092564

Shi, S., Jiang, L., Deng, J., Wang, Z., Guo, C., Shi, J. ...Li, H. (2022). PV-RCNN++: Point-Voxel Feature Set Abstraction With Local Vector Representation for 3D Object Detection. *Int. J. Comput. Vision*, *131*(2), 531-551. https://doi.org/10.1007/s11263-022-01710-9

Visionary-T - Archive | SICK. (n.d.). https://www.sick.com/tr/en/archive/visionary-t/c/g358152

Zhou, Y., & Tuzel, O. (2018). VoxelNet: End-to-End Learning for Point Cloud Based 3D Object Detection. *2018 IEEE/CVF Conference on Computer Vision and Pattern Recognition*, 4490-4499. https://doi.org/10.1109/CVPR.2018.00472

Biographies

FARUK AHMED is an assistant professor of engineering technology at the University of Memphis, where he earned both his MS and PhD degrees in engineering. His research focuses on assistive technology, human-computer interaction, machine learning, computer vision, and adaptive instructional systems. Dr. Ahmed may be reached at mfahmed@memphis.edu

KEVIN BERISSO is the director of the AutoID lab at the University of Memphis. He has been teaching within the AutoID industry for over 20 years, is a member of the AIDC 100, and has been awarded the Ted Williams award by AIM Inc., for his work in the industry. He is a regular presenter at RFID Journal Live and has worked with GS1 on barcode research as well as having been involved in RFID research for returnable transport items in the automotive industry and tagging items in the aerospace industry. Dr. Berisso may be reached at kberisso@memphis.edu

Optimization of FDM Process Parameters for Tensile Strength Using Machine Learning and Evolutionary Algorithms

Jayson Francois, Florida A&M University; Shonda Bernadin, Florida A&M University

Abstract

In this study, the authors examined a data-driven approach for enhancing the tensile properties of ABS components manufactured via fused deposition modeling (FDM). Test specimens were printed using systematically varied combinations of extrusion temperature, layer thickness, and infill density. The resulting tensile data were then used to train several regression models. Among the approaches examined, gradient boosting, support vector regression, and polynomial regression proved to be the most dependable, each accounting for more than eighty-six percent of the variation in measured strength. These trained models were then paired with evolutionary optimization methods to search for printing conditions that would yield higher-performing parts. Multiple optimizers converged on parameter regions associated with predicted tensile strengths in the upper 30-megapascal range.

To provide a physical reference point for these predictions, a finite element model of the ISO-527-5A specimen was built in COMSOL. The simulated tensile response reproduced the expected stress distribution in the gauge section and indicated a failure load consistent with both the machine learning estimates and the manufacturer's reported properties. While the optimized parameter sets could not be fabricated within the project timeline, the close agreement between simulations, model predictions, and known material behavior supports the reliability of the proposed workflow. The results highlight the usefulness of integrating supervised learning, optimization, and finite-element analysis to guide FDM process decisions and demonstrate the potential for extending this approach to applications requiring more complex mechanical or functional performance criteria.

Introduction

Additive manufacturing (AM) has significantly reshaped modern fabrication methods, with FDM emerging as one of the most widely adopted techniques. Its strengths lie in enabling customized designs, rapid prototyping, and the economical production of intricate geometries. Among the performance factors of FDM, tensile strength remains especially important, since it determines whether a part can endure load-bearing conditions and maintain structural reliability. Establishing reliable predictive models for tensile strength can support improvements in process design, material selection, and quality assurance (Braconnier, Jensen & Peterson, 2020). Prior studies showed that correlating process inputs—ranging from temperature control to part dimensions and build orientation—with final part behavior led to measurable gains in mechanical performance (Oleff, Küster, Stonis & Overmeyer, 2021). In extrusion-based AM, predictive approaches now play a central role in helping manufacturers anticipate performance outcomes, minimize production costs, and shorten lead times.

However, experimentation continues to dominate research, mainly because of the challenges posed by high-dimensional parameter spaces, where isolating the effect of individual variables is difficult (Ramos, Angel, Siqueiros, Sahagun, Gonzalez & Ballesteros, 2025). The repeated heating and cooling inherent in FDM often weakens interlayer bonding and creates inconsistencies in part strength, adding further complexity. These nonlinear behaviors limit the accuracy of conventional regression models. In addition, most predictive frameworks neglect the time-dependent nature of FDM processes, which frequently results in models that fail to capture important dynamics (Alli et al., 2024). This has led to a shift toward data-driven methods, where machine learning (ML) techniques and genetic algorithms can identify hidden patterns and efficiently optimize parameter settings.

In this current study, the authors developed a framework for forecasting tensile strength in FDM by examining process factors such as infill density, infill geometry, extrusion temperature, and layer thickness control. Genetic algorithms were applied to enhance optimization within single-objective design problems, even when multiple functional requirements were present. Together, these methods provide a pathway to developing stronger, more reliable FDM parts, while reducing trial-and-error effort and improving overall production efficiency.

Literature Review

In the past, researchers optimized AM parameters mostly through trial-and-error experiments or regression-based statistical tools such as analysis of variance (ANOVA) and response surface methodology (RSM). Although these approaches yielded some insights, they struggled to account for nonlinear interactions between process variables (Malashin, Martysyuk, Tynchenko, Nelyub, Borodulin & Galinovsky, 2024). The rise of supervised ML has changed this landscape by providing new ways to link process conditions with material performance. Early investigations used methods such as random forest (RF), gradient boosting, and

decision trees to estimate properties such as tensile strength, elongation, and Young's modulus (Abdalla et al., 2024). One advantage of these models is their ability to make reasonable predictions even when the dataset is incomplete. For instance, Shan, Gao, Rao, Wu, Yan, and Bi (2024) used a random forest algorithm to forecast the mechanical behavior of components fabricated through selective laser sintering and reported higher accuracy compared to conventional regression.

Other supervised learning methods have also found applications in AM research. support vector machines are often used for ranking and classifying parts by analyzing how process settings affect performance. Artificial neural networks (ANNs), on the other hand, excel at detecting temporal relationships across different stages of production. Studies by Manoharan, Chockalingam, and Ram (2020) and Muhamedagic, Berus, Potočnik, Cekic, Begic-Hajdarevic, Cohodar Husic, and Ficko (2022) demonstrated that ANN models could successfully connect FDM parameters (e.g., layer thickness, raster angle, and build orientation) to mechanical outcomes, including tensile, compressive, and flexural strength. Taken together, these findings highlight that neural networks generally surpass other supervised approaches in capturing nonlinear dependencies and delivering stronger predictive accuracy.

ML techniques have shown that parts produced through AM generally retain their structural integrity, without signs of compaction, scaling, or loss of resolution introduced during the printing process. However, only a limited number of studies have attempted to estimate tensile strength using regression-based ML approaches in relation to FDM parameters. For example, Anand and Satyarthi (2024) and Tura, Lemu, and Mamo (2022) applied feed-forward neural networks to evaluate how raster orientation, air gap, and build direction influence tensile properties. Their findings suggest that careful parameter selection, supported by ML, can significantly improve the reliability of printed parts.

In recent years, the rise of deep learning has further improved predictive accuracy. For instance, convolutional neural networks (CNNs) have been used to handle regression tasks by incorporating process data such as pulse waveforms, temperature variations, and layer deposition sequences (Ding, Hou, Wang, Cui, Yu & Wilson, 2025). Although still relatively new, these applications indicate a shift toward more advanced methods for capturing the complex, time-dependent behavior of FDM processes. Alongside prediction, many researchers combine ML with optimization techniques to identify parameter values that enhance material performance. Genetic algorithms (GA), particle swarm optimization, and Bayesian optimization are among the most common tools used with ML models. For example, Boppana and Ali (2024) and Deshwal, Kumar, and Chhabra (2020) proposed a hybrid ANN–GA approach to predict and optimize the tensile strength of FDM-produced ABS parts. By iteratively refining the model with new experimental results, the genetic algorithm improved its accuracy and provided more reliable guidance on parameter adjustments.

Gathering dependable datasets remains one of the biggest obstacles to using ML in advanced manufacturing. Zihao, Hongyuan, Pengyu, Weidong, Ji, and Fuhua (2022) pointed out that, because data are often incomplete or poorly labeled, many models are trained for only one machine or material system, limiting their broader use. Researchers have tried to get around these issues by combining strategies—borrowing from engineering practices, drawing on prior studies, and adding new data sources—to make their models more adaptable. In some cases, similarities between materials can also help; for instance, because polycarbonate and polyethylene share comparable properties, a model trained for one can sometimes be applied to the other (Al-Zaidi & Al-Gawhari, 2023).

Even with these advances, there are still important gaps. Temperature changes within layers, which are believed to play a role in damage formation, are rarely studied in detail. Many models also work under the assumption that input conditions stay constant from year to year, which does not reflect reality. Xie, Sun, and Zhao (2025) stressed that having larger and better-quality datasets would allow researchers to run more experiments and check their results more effectively. Another direction drawing attention is explainable AI (XAI). Since ML models often act like "black boxes," judging which ones perform best is difficult. Adding explanation features would improve trust and give users more insight into how a system or robot is functioning. Random forest is an ensemble method that builds on decision trees and has been applied with good results in predicting material properties for AM (Raymaekers, Rousseeuw, Servotte, Verdonck & Yao, 2025). Because it averages the output of many trees, it helps reduce the overfitting that usually occurs when a single decision tree is used. Another strength of the method is its ability to handle datasets that include several interacting variables, which makes it suitable for studies of FDM, where many process parameters come into play.

Even with these strengths, random forest (RF) is not without its drawbacks. Hassan, Salem, Bailek, and Kisi (2023) pointed out that it does not fully capture the layered structure that is central to FDM printing. Ensemble models like RF also tend to assume that input features are independent from one another, which is often not the case in processes that evolve over time. Authors from two other studies noted that this assumption can lead to reduced accuracy when RF is used to study the temporal behavior of AM systems (Mishra, Tripathi, Chaurasia & Chaurasia, 2025; Shrivastav & Kumar, 2021). Deep learning, a subset of ML built on artificial neural networks, has become an important tool for predicting material properties in AM. These models effectively capture straightforward and complex patterns in AM processes. In practice, four main architectures have been applied in this area: autoencoders, deep belief networks (DBNs), CNNs, and recurrent neural networks (RNNs).

Autoencoders are unsupervised models designed to compress input data into simpler forms and reconstruct them (Berahmand, Daneshfar, Salehi, Li & Xu, 2024). In AM, they reduce the dimensionality of large datasets, making it easier for supervised models to handle property prediction. For example, autoencoders have been applied to thermographic images and sensor data, compressing them into latent features that support defect detection and print-quality analyses (Gbadamosi-Adeniyi, Ferguson & Horn, 2025). Deep belief networks, which are built from stacked restricted Boltzmann machines, have shown promise in learning hierarchical features. They can capture relationships among parameters such as print speed, layer height, and temperature (Alzubaidi et al., 2021). While they are not as common as CNNs or RNNs, DBNs link simpler networks and more advanced deep learning methods.

CNNs are the most widely used deep learning approach in AM because of their strength in image analysis. They process layer snapshots, thermographic images, or surface scans to identify problems such as delamination, roughness, or internal defects (Yangue, Ye, Kan & Liu, 2023). CNNs are also helpful for predicting material properties from post-print microstructure images as they excel at extracting spatial details. RNNs and improved versions such as long short-term memory networks are designed to handle time-dependent data (Mienye, Swart & Obaido, 2024). In AM, they have been applied to model how temperature changes, extrusion speed, and cooling conditions influence part quality as the printing process unfolds. This ability to capture sequential effects makes them well-suited for tasks that static models cannot address.

FDM has become important in many industries because it can create complex designs and customized components while reducing waste (Zhou et al., 2024). However, the quality of an FDM print depends heavily on process conditions. Variables such as print speed, infill, layer thickness, nozzle temperature, and the arrangement of paths determine how strong and accurate the final part will be (Taqdissillah, Muttaqin, Darsin, Dwilaksana & Ilminnafik, 2022). Selecting these parameters is not straightforward, but performance improves significantly when they are chosen carefully. Earlier, optimization was carried out mainly through trial-and-error testing and statistical approaches such as Taguchi methods or RSM (Kozik et al., 2019). These methods produced valuable insights but also required considerable time and cost and often failed to account for thermal or stress interactions between layers. To address such limitations, researchers began using metaheuristic techniques. Approaches such as GAs, PSO, and simulated annealing have been employed to search for parameter settings that improve strength or reduce defects such as porosity and warping (Fadhil, 2025; Rajwar, Deep & Das, 2023). GAs are especially suited to problems that do not have a single best answer, enabling engineers to make better choices for layer height, raster angle, and part orientation.

More recently, optimization in AM has moved toward data-driven approaches. ML models such as random forests, gradient boosting, and deep neural networks can predict mechanical properties based on input conditions (Airlangga & Liu, 2025; Nadkarni, Vijay & Kamath, 2023). These models can act as surrogates for experiments, meaning that not every possible setting needs to be tested physically. This has made it easier to evaluate trade-offs in design. For example, Pareto optimization can balance competing requirements such as strength versus production speed (Haleem, Javaid, Rab, Singh, Suman & Kumar, 2023). Together, these advances show how the focus of AM optimization has shifted from labor-intensive testing to faster, data-driven methods.

Methodology

In this current study, the authors implemented a closed-loop optimization framework integrating experimental characterization, ML prediction, and algorithmic optimization to maximize the tensile strength of 3D-printed ABS components fabricated via FDM. The methodology was composed of three primary stages: 1) data collection through physical testing, 2) regression model development, and 3) single-objective optimization using multiple evolutionary strategies. Twenty-seven tensile specimens were fabricated using a commercial ABS filament and printed using FDM under varied process parameters. The input variables included extrusion temperature (°C), layer thickness (mm), and infill percentage (%). Table 1 summarizes the FDM process parameters used for case studies on material part properties. Figure 1 shows the ISO 527 5A standards by which specimens were printed. Figure 2 shows the universal testing machine used to measure tensile strength. This dataset served as the training set for subsequent ML model development.

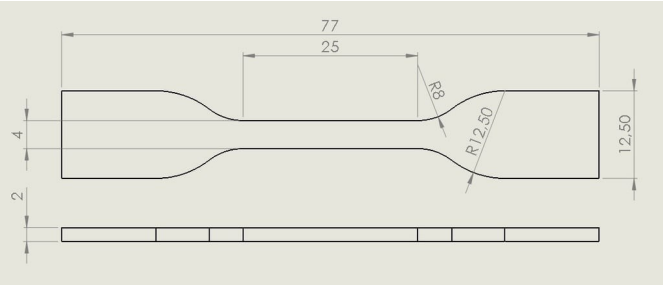

Figure 1. Tensile testing sample type 5A of the ISO-527 standards.

Five supervised regression models were trained to predict tensile strength from process parameters: gradient boosting regressor (GBR) (Figure 3), support vector regression (SVR), polynomial regression (PR) (degree 2), linear regression (LR), and random forest regressor. The dataset was split into training and testing subsets using an 80/20 split. Model performance was evaluated using R^2 score, mean absolute error (MAE), and root mean squared error (RMSE). Cross-validation was applied to assess model

Table 1. FDM process parameters used for case studies on material part properties.

References	Material	Parameters	Findings	Gaps
Alhazmi & Backar (2020)	PLA	Infill density, nozzle temperature, rater width	Both infill density and raster orientation had influence on tensile strength and Young's modulus.	Limited to PLA, effects of extrusion temperature, layer thickness or nozzle diameter explored, no predictive modeling.
Özkül, Kuncan & Ulkir (2025)	ABS	Layer thickness, Infill density, nozzle temperature	Infill density was the dominant factor for tensile strength; layer thickness primarily affected surface roughness.	No optimization algorithm was applied; study focused solely on prediction. No validation using independent samples outside the experimental design.
Popescu, Zapciu, Amza, Baciu & Marinescu (2018)	ABS, PLA, Nylon	Layer thickness, raster angle, build orientation, infill density, nozzle diameter, print speed	Layer thickness and raster angle had the strongest influence on tensile strength; lower layer thickness produced higher strength.	No predictive modeling or optimization used; results are not generalized across materials; study lacked integrated physics-based or ML-based analysis.
Sood, Ohdar & Mahapatra (2010)	ABS	Layer thickness, build orientation, raster angle, raster width, air gap	All five parameters significantly influenced mechanical performance.	Focused solely on process–property modeling; did not incorporate machine-learning prediction methods.
Ulkir, Ertugrul, Ersoy & Yağımlı (2024)	ABS	Nozzle temperature	Higher nozzle temperatures caused significant loss in mass, decreased tensile strength, reduced hardness, and increased dimensional errors for thickness.	Only one parameter studied (temperature); no multi-parameter interaction effects analyzed. Did not explore optimization or predictive modeling.

generalizability. The best-performing models (GBR, SVR, and POLY) were selected for use in the optimization loop. Five single-objective optimization algorithms were implemented to identify the optimal combination of FDM parameters that maximized predicted tensile strength: differential evolution, GA, Nelder Mead, pattern search, and evolution strategy.

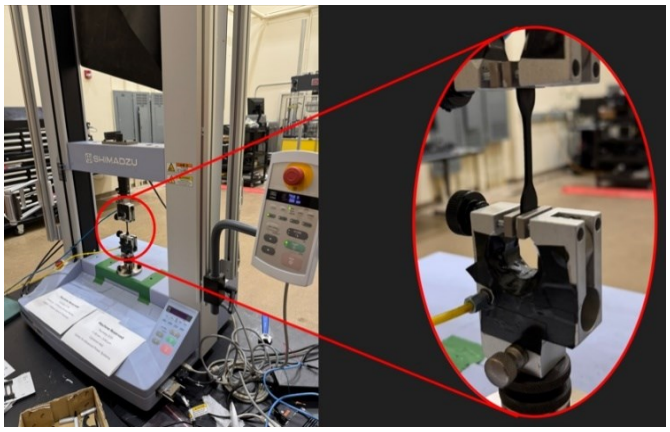

Figure 2. Tensile strength measurement machine.

Each algorithm was executed with bounds defined by the physical printer's capabilities and material limitations. The objective function maximized the predicted tensile strength as forecasted by the selected ML models. The output of each optimizer was a set of optimal parameters that were then passed through all five trained regression models to compare predicted performance. For model validation, previously fabricated tensile specimens using older optimization outputs were used to compare predicted versus actual tensile strength. These comparisons helped evaluate model accuracy and inform the trustworthiness of predictions for new, untested parameter sets.

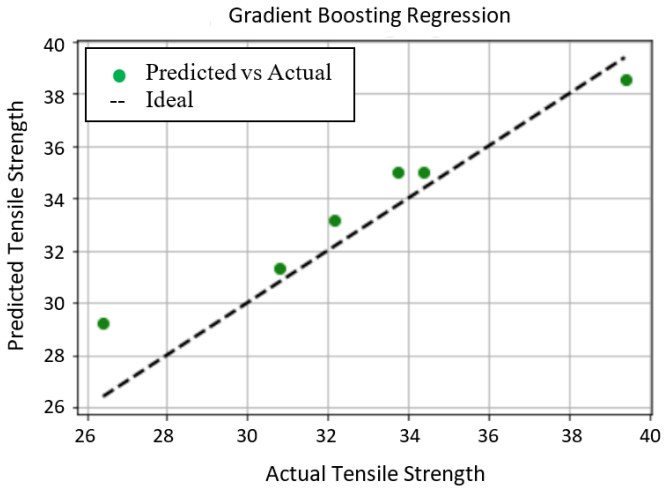

Figure 3. Gradient boosting regression training and verification.

Results

Table 2 summarizes the performance of five regression models using the R^2 score, MAE, and RMSE. Among these, GBR and PR achieved the highest R^2 scores (~0.87) and the lowest error values, indicating superior predictive accuracy. In contrast, linear regression exhibited the weakest performance, with the lowest R^2 and the highest MAE and RMSE, suggesting that it failed to capture the non-linear relationships inherent in the data. These results underscore the importance of employing non-linear models in capturing the complexities of the FDM process.

Table 2. Performance metrics for regression models.

Prediction models	R^2 Score	MAE score	RMSE
Random forest regressor	0.757942	1.696735	1.927416
Gradient boosting regressor	0.870883	1.176535	1.407687
Support vector regression	0.867693	1.193759	1.424975
Linear regression	0.583917	2.398614	2.527003
Polynomial regression	0.870912	1.176341	1.407533

Table 3 presents the optimal process parameters—extrusion temperature, layer thickness, and infill percentage—identified by each single-objective optimization algorithm. Notably, pattern search selected the lowest temperature (235°C) and highest infill (50%), whereas evolutionary strategy found a much lower infill requirement (23.60%) while maintaining a high temperature. The variability of optimal parameters across algorithms reflects the divergent search strategies and local versus global exploration characteristics of each optimizer. These differences matter because they can lead to significantly different material usage, energy consumption, and, ultimately, mechanical properties in the printed part. Optimizers that balance exploration (e.g., differential evolution and evolutionary strategy) tend to yield more-efficient solutions.

Table 3. Optimal process parameters for maximum tensile strength.

Single-objective optimization models	Temperature (°C)	Thickness (mm)	Infill (%)
Genetic algorithm	251.62	0.142	34.55
Differential evolution	247.79	0.206	38.11
Evolutionary strategy	251.62	0.202	23.60
Nelder Mead	253.24	0.198	48.17
Pattern search	235.00	0.200	50.00

Table 4 shows the predicted tensile strengths generated by each ML model using the optimal parameters identified in Table 2. Across all optimizers, gradient boosting and polynomial regression consistently produced the highest predictions, particularly when paired with parameters from evolutionary strategy and differential evolution. These results suggest strong synergy between these optimizers and non-linear regression models. Conversely, pattern search yielded the lowest predicted strengths across all models, likely due to its local search nature, which may have caused it to converge prematurely on suboptimal parameter sets. These differences are important because they inform which combinations of optimizers and regressors are most likely to approach or exceed real-world performance requirements, especially when physical validation is limited.

Table 4. Tensile strength prediction based on optimization algorithms.

Optimization Algorithms	RF (MPa)	GBR (MPa)	SVR (MPa)	LR (MPa)	PR (MPa)
Genetic algorithm	36.64	38.52	37.01	35.61	37.76
Differential evolution	36.71	38.56	38.14	35.89	37.67
Evolutionary strategy	36.71	38.56	38.46	36.10	38.44
Nelder Mead	36.01	36.12	37.71	36.08	37.40
Pattern search	35.12	35.03	34.73	35.26	35.40

Figure 4 shows the ISO-527-5A dog-bone specimen used in the simulations. Its reduced gauge section was designed so that the highest stresses—and eventual failure in real testing—occurred in a predictable, centralized region. Using this same geometry throughout the parameter sweeps made it possible to compare printed samples, experimental data, and FEM predictions on equal footing, while examining how different printing settings influenced the stress response. Figure 5 is the contour plot of the von Mises stress field in the tensile specimen when a 1600N load is applied. The analysis revealed the expected concentration of stress in the narrow middle section, while the areas near the grips remained comparatively low due to their greater stiffness. The distribution confirmed that the simulated loading behaved as it would in a physical test and that the optimized parameters led to a realistic mechanical response.

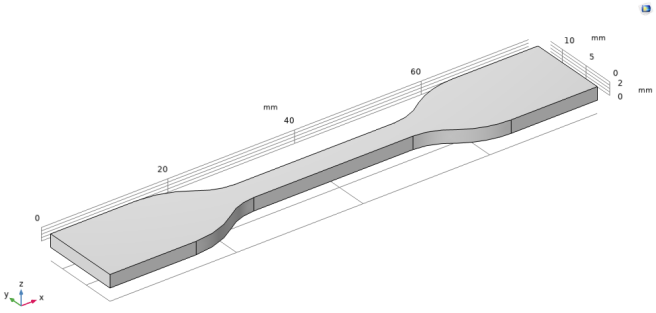

Figure 4. Geometry of the ISO 527-5A tensile test specimen.

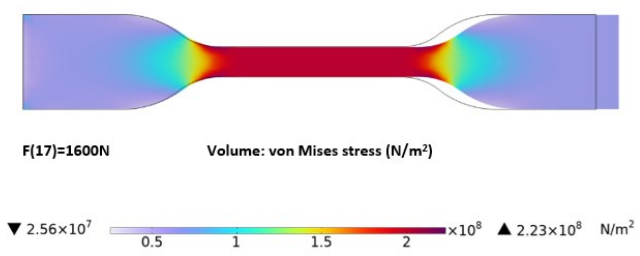

Figure 5. von Mises stress distribution (contour plot).

Figure 6 displays how the von Mises stress changed along the length of the specimen for several increasing load levels. Each curve represents one step in the load sequence. The central portion of the specimen maintained a level stress profile, whereas the transitions near the shoulders introduced noticeable gradients. These patterns offer a reference for judging how well predicted tensile-strength values match the mechanical behavior captured in the simulations.

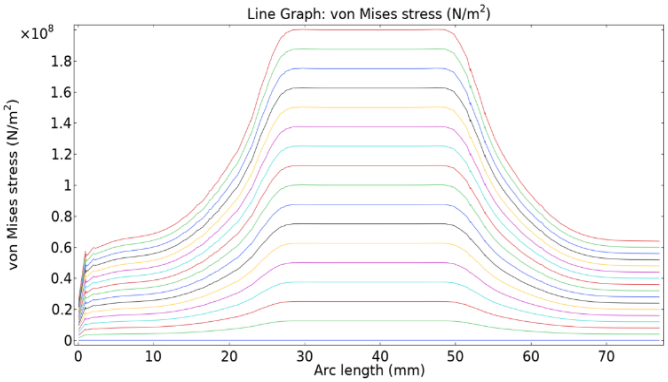

Figure 6. von Mises stress along the specimen length (line plot).

Figure 7 tracks the highest von Mises stress in the specimen as the applied tensile force increased. The almost straight-line relationship reflects the primarily elastic response within the simulated load range. By comparing these stress values with known material strength limits, the curve helps bridge the simulation results with the tensile-strength predictions derived from the optimized printing parameters.

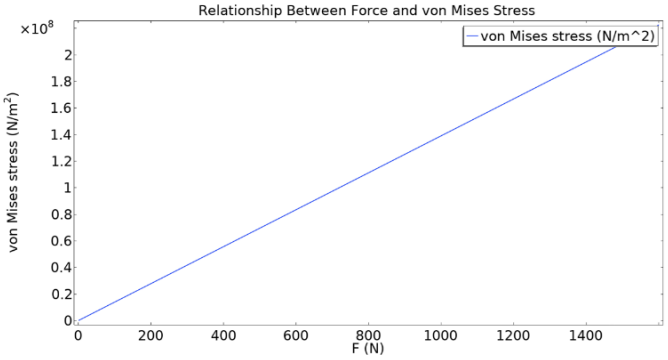

Figure 7. Relationship between applied force and maximum von Mises stress.

Discussion

The results of this project demonstrated that combining machine learning models with optimization techniques can effectively enhance the tensile performance of ABS parts produced through FDM. Among the five regression approaches tested, the GBR and the polynomial regression model were the strongest performers. Both models achieved R^2 values close to 0.87 and produced the lowest prediction errors. Although gradient boosting is typically considered the more advanced method, the polynomial model performed almost as well. This was mainly due to the interaction and curvature features introduced during preprocessing, such as the temperature-multiplied-by-thickness term and the squared thickness feature. These engineered inputs captured much of the nonlinear behavior directly, which allowed the polynomial model to represent the main physical relationships in the data without requiring the complexity of a boosted ensemble. In relatively small datasets, thoughtful feature engineering can reduce the advantage commonly held by more sophisticated models and prevent them from overfitting.

The optimization algorithms examined in this study generated a recommended set of printing conditions for each. Although they used very different search strategies, the predictions from the top regression models were consistently aligned with one another. Differential evolution and evolution strategy produced the highest estimated strengths, both near 38.5 megapascals, and the GA delivered values that were only slightly lower. The fact that several different methods converged on a similar region of the parameter space suggests that these conditions genuinely represent a high-performing combination rather than a result of model-specific behavior. In contrast, pattern search regularly produced weaker parameter sets. Across all five regression models, the tensile strengths predicted for the conditions selected by pattern search were consistently near the bottom of the range. This is consistent with the nature of the algorithm, which tends to explore only a local area and can easily become stuck in a suboptimal region. The specific settings it returned, such as the lower extrusion temperature, were also not typical of conditions that promote strong bond formation between layers in FDM parts.

To provide a physics-based reference point for the ML predictions, a finite element model of the ISO 527 5A tensile specimen was created in COMSOL. The geometry used in the physical tensile tests was reproduced and the printed ABS material was assigned its measured elastic properties, including a Young's modulus of about 1.96 gigapascals and a Poisson's ratio of 0.35. A simple von Mises elastoplastic formulation was used and tensile loads up to approximately 1600 newtons were applied. The resulting stress distribution behaved as expected, with the highest values occurring in the narrow-gauge region and a nearly linear increase in stress with applied force. When the simulated stresses were compared with the manufacturer's

reported tensile strength of roughly forty megapascals, the model indicated that yielding would begin between about 700 and 750 newtons. This estimate is very close to the 37 to 38 megapascals predicted by the strongest ML models for the optimized printing conditions. The close agreement between the finite element simulation, the ML predictions, and the known material properties is an important validation step. It shows that the optimized parameter sets identified through the predictive framework correspond to physically realistic behavior and are not artifacts of the modeling process. This agreement increases confidence in the overall optimization strategy, even though the new specimens derived from the final parameter sets were unable to be printed and tested within the project period.

The modest size of the experimental dataset presented another challenge. Even though the sample count was limited, the combination of careful feature engineering and cross-validation helped the models avoid overfitting and achieve reliable performance within the studied parameter ranges. A larger dataset would likely increase the stability and generalizability of the predictions, and future work may benefit from active learning or structured experimental design to collect additional samples in areas where model uncertainty is highest. Ultimately, this study focused solely on maximizing tensile strength. Many real applications of FDM, especially those involving materials that must dissipate static charge, require a balance of mechanical, electrical, and thermal properties. The framework demonstrated here can be extended to support proper multi-objective optimization, making it useful for advanced design tasks where multiple performance criteria must be satisfied simultaneously.

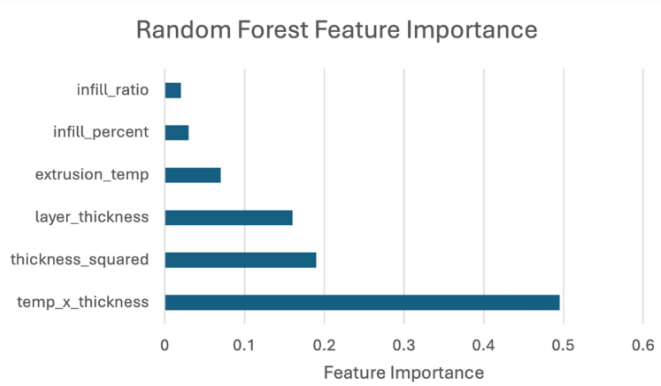

Figure 8. Feature important derived from the random forest regressor.

Conclusions

From this study, the authors confirmed that pairing ML with evolutionary search methods provides an efficient approach to enhancing the tensile performance of ABS components produced by FDM. Instead of relying on repeated trial and error, the combined approach used predictive models to explore the printing parameter space in a targeted manner. Among the regression models evaluated, gradient boosting, polynomial regression, and support vector regression provided the most accurate estimates of tensile strength, each explaining more than eighty-six percent of the variance in the experimental data. The close performance of the polynomial model, which benefited from carefully engineered interaction and curvature features, highlights the value of incorporating domain knowledge directly into the feature set. Several of the optimization algorithms converged on similar combinations of extrusion temperature, layer thickness, and infill density. Differential evolution, evolution strategy, and the GA consistently produced parameter sets associated with tensile strengths in the upper thirty megapascal range. The agreement among the strongest regression models for these solutions increases confidence that the identified conditions represent meaningful optima rather than artifacts of a specific algorithm. Pattern search was the one method that produced weaker results, which reflects its limited ability to explore the entire parameter landscape.

To provide a mechanical point of reference for the ML predictions, a finite element model of the ISO 527 5A tensile specimen was developed in COMSOL. The simulation reproduced the expected stress concentration in the gauge region and predicted the onset of yielding at a load of approximately 700 to 750 Newtons. This corresponds to a tensile strength of thirty-eight to forty megapascals, which matches the predictions generated by the top regression models. The close agreement between the simulation results and the model predictions indicates that the optimized parameter sets are mechanically realistic rather than numerical artifacts. This consistency strengthens the overall framework by linking statistical inference with a physics-based representation of material behavior. Although the newly identified parameter sets could not be fabricated and tested within the project period, the agreement among multiple regression models, the measured material properties, and the finite element results helps mitigate this limitation. Additional experiments would further enhance confidence in the predictions, and future work could utilize active learning or structured experimental design to expand the dataset more strategically.

The framework developed here focused on tensile strength; however, many functional applications, especially those involving ESD-safe materials, require a balance of electrical, thermal, and mechanical characteristics. The same workflow can be extended to a multi-objective setting, allowing designers to identify printing conditions that deliver the best overall combination of performance metrics. These findings offer practical value for industrial environments where stronger and more reliable polymer components are needed. By reducing the amount of experimental testing required to achieve high-performance settings, the approach can contribute to more efficient and consistent AM processes.

References

Abdalla, Y., Ferianc, M., Awad, A., Kim, J., Elbadawi, M., Basit, A. W. …Rodrigues, M. (2024). Smart laser Sintering: Deep Learning-Powered powder bed fusion 3D printing in precision medicine. *International Journal of Pharmaceutics, 66*1, 124440. https://doi.org/10.1016/j.ijpharm.2024.124440

Airlangga, G., & Liu, A. (2025). A Hybrid Gradient Boosting and Neural Network Model for Predicting Urban Happiness: Integrating Ensemble Learning with Deep Representation for Enhanced Accuracy. *Machine Learning and Knowledge Extraction, 7*(1), 4. https://doi.org/10.3390/make7010004

Alhazmi, M., & Backar, A. (2020). Influence of infill density and orientation on the mechanical response of PLA+ specimens produced using FDM 3D printing. *International Journal of Advanced Science and Technology, 29* (6), 3362-3371.

Alli, Y. A., Anuar, H., Manshor, M. R., Okafor, C. E., Kamarulzaman, A. F., Akçakale, N. …Mohd Nasir, N. A. (2024). Optimization of 4D/3D printing via machine learning: A systematic review. *Hybrid Advances, 6*, 100242. https://doi.org/10.1016/j.hybadv.2024.100242

Al-Zaidi, A. A. M. A., & Al-Gawhari, F. J. J. (2023). Types of Polymers Using in 3D Printing and Their Applications: A Brief Review. *European Journal of Theoretical and Applied Sciences, 1*(6), 978-985. https://doi.org/10.59324/ejtas.2023.1(6).94

Alzubaidi, L., Zhang, J., Humaidi, A. J., Al-Dujaili, A., Duan, Y., Al-Shamma, O. …Farhan, L. (2021). Review of deep learning: Concepts, CNN architectures, challenges, applications, future directions. *Journal of Big Data, 8*(1), 53. https://doi.org/10.1186/s40537-021-00444-8

Anand, S., & Satyarthi, M. K. (2024). Neural network-based modeling of FFF process for PET-G: Evaluating MLPNN and RBFNN performance in mechanical property prediction. Proceedings of the Institution of Mechanical Engineers, Part E. *Journal of Process Mechanical Engineering*, 09544089241272752. https://doi.org/10.1177/09544089241272752

Berahmand, K., Daneshfar, F., Salehi, E. S., Li, Y., & Xu, Y. (2024). Autoencoders and their applications in machine learning: A survey. *Artificial Intelligence Review, 57*(2), 28. https://doi.org/10.1007/s10462-023-10662-6

Boppana, V. C., & Ali, F. (2024). Improvement of tensile strength of fused deposition modelling (FDM) part using artificial neural network and genetic algorithm techniques. *International Journal of Industrial Engineering and Operations Management, 6*(2), 117-142. https://doi.org/10.1108/IJIEOM-01-2023-0006

Braconnier, D. J., Jensen, R. E., & Peterson, A. M. (2020). Processing parameter correlations in material extrusion additive manufacturing. *Additive Manufacturing, 31*, 100924. https://doi.org/10.1016/j.addma.2019.100924

Deshwal, S., Kumar, A., & Chhabra, D. (2020). Exercising hybrid statistical tools GA-RSM, GA-ANN and GA-ANFIS to optimize FDM process parameters for tensile strength improvement. *CIRP Journal of Manufacturing Science and Technology, 31*, 189-199. https://doi.org/10.1016/j.cirpj.2020.05.009

Ding, H., Hou, H., Wang, L., Cui, X., Yu, W., & Wilson, D. I. (2025). Application of Convolutional Neural Networks and Recurrent Neural Networks in Food Safety. *Foods, 14*(2), 247. https://doi.org/10.3390/foods14020247

Fadhil, H. (2025, February 4). *Metaheuristic Algorithms in Optimization and its Application: A Review* [Conference presentation]. Proceedings of the 3rd International Conference on Engineering and Innovative Technology. The 3rd International Conference on Engineering and Innovative Technology. https://doi.org/10.31972/iceit2024.013

Gbadamosi-Adeniyi, T., Ferguson, S., & Horn, T. (2025). Deep learning-based real-time monitoring of electron beam powder bed fusion (EB-PBF) via electron emission. *Journal of Intelligent Manufacturing*. https://doi.org/10.1007/s10845-025-02598-1

Haleem, A., Javaid, M., Rab, S., Singh, R. P., Suman, R., & Kumar, L. (2023). Significant potential and materials used in additive manufacturing technologies towards sustainability. *Sustainable Operations and Computers, 4*, 172-182. https://doi.org/10.1016/j.susoc.2023.11.004

Hassan, M. A., Salem, H., Bailek, N., & Kisi, O. (2023). Random Forest Ensemble-Based Predictions of On-Road Vehicular Emissions and Fuel Consumption in Developing Urban Areas. *Sustainability, 15*(2), 1503. https://doi.org/10.3390/su15021503

Kozik, V., Barbusinski, K., Thomas, M., Sroda, A., Jampilek, J., Sochanik, A. …Bak, A. (2019). Taguchi Method and Response Surface Methodology in the Treatment of Highly Contaminated Tannery Wastewater Using Commercial Potassium Ferrate. *Materials, 12*(22), 3784. https://doi.org/10.3390/ma12223784

Malashin, I., Martysyuk, D., Tynchenko, V., Nelyub, V., Borodulin, A., & Galinovsky, A. (2024). Mechanical Testing of Selective-Laser-Sintered Polyamide PA2200 Details: Analysis of Tensile Properties via Finite Element Method and Machine Learning Approaches. *Polymers, 16*(6), 737. https://doi.org/10.3390/polym16060737

Manoharan, K., Chockalingam, K., & Ram, S. S. (2020, August 7-9). Prediction of tensile strength in fused deposition modeling process using artificial neural network technique. *Proceedings of the 3rd International Conference on Frontiers in Automobile and Mechanical Engineering (FAME), 23*(1), 080012, Chennai, India. https://doi.org/10.1063/5.0034016

Mienye, I. D., Swart, T. G., & Obaido, G. (2024). Recurrent Neural Networks: A Comprehensive Review of Architectures, Variants, and Applications. *Information, 15* (9), 517. https://doi.org/10.3390/info15090517

Mishra, D., Tripathi, S. M., Chaurasia, A., & Chaurasia, P. K. (2025). A Review on Ensemble Learning Methods:

Machine Learning Approach. *International Journal of Research Publication and Reviews, 6*(2), 3795-3803. https://doi.org/10.55248/gengpi.6.0225.0971

Muhamedagic, K., Berus, L., Potočnik, D., Cekic, A., Begic -Hajdarevic, D., Cohodar Husic, M., & Ficko, M. (2022). Effect of Process Parameters on Tensile Strength of FDM Printed Carbon Fiber Reinforced Polyamide Parts. *Applied Sciences, 12*(12), 6028. https://doi.org/10.3390/app12126028

Nadkarni, S. B., Vijay, G. S., & Kamath, R. C. (2023). Comparative Study of Random Forest and Gradient Boosting Algorithms to Predict Airfoil Self-Noise. *Engineering Proceedings*, *59*(1), 24. https://doi.org/10.3390/engproc2023059024

Oleff, A., Küster, B., Stonis, M., & Overmeyer, L. (2021). Process monitoring for material extrusion additive manufacturing: A state-of-the-art review. *Progress in Additive Manufacturing, 6*(4), 705-730. https://doi.org/10.1007/s40964-021-00192-4

Özkül, M., Kuncan, F., & Ulkir, O. (2025). Predicting mechanical properties of FDM-produced parts using machine learning approaches. *Journal of Applied Polymer Science, 142*, e56899. https://doi.org/10.1002/app.56899

Popescu, D., Zapciu, A., Amza, C., Baciu, F., & Marinescu, R. (2018). FDM process parameters influence over the mechanical properties of polymer specimens: A review. *Polymer Testing, 69*, 157-166.

Rajwar, K., Deep, K., & Das, S. (2023). An exhaustive review of the metaheuristic algorithms for search and optimization: Taxonomy, applications, and open challenges. *Artificial Intelligence Review, 56*(11), 13187-13257. https://doi.org/10.1007/s10462-023-10470-y

Ramos, A., Angel, V. G., Siqueiros, M., Sahagun, T., Gonzalez, L., & Ballesteros, R. (2025). Reviewing Additive Manufacturing Techniques: Material Trends and Weight Optimization Possibilities Through Innovative Printing Patterns. *Materials, 18*(6), 1377. https://doi.org/10.3390/ma18061377

Raymaekers, J., Rousseeuw, P. J., Servotte, T., Verdonck, T., & Yao, R. (2025). A Powerful Random Forest Featuring Linear Extensions (RaFFLE) (Version 1). arXiv. https://doi.org/10.48550/ARXIV.2502.10185

Shan, X., Gao, C., Rao, J. H., Wu, M., Yan, M., & Bi, Y. (2024). Experimental Study and Random Forest Machine Learning of Surface Roughness for a Typical Laser Powder Bed Fusion Al Alloy. *Metals, 14*(10), 1148. https://doi.org/10.3390/met14101148

Shrivastav, L. K., & Kumar, R. (2021). An Ensemble of Random Forest Gradient Boosting Machine and Deep Learning Methods for Stock Price Prediction. *Journal of Information Technology Research, 15*(1), 1-19. https://doi.org/10.4018/JITR.2022010102

Sood, A. K., Ohdar, R. K., & Mahapatra, S. S. (2010). Parametric appraisal of mechanical property of fused deposition modelling processed parts. *Materials & Design, 31*(1), 287-295.

Taqdissillah, D., Muttaqin, A. Z., Darsin, M., Dwilaksana, D., & Ilminnafik, N. (2022). The Effect of Nozzle Temperature, Infill Geometry, Layer Height and Fan Speed on Roughness Surface in PETG Filament. *Journal of Mechanical Engineering Science and Technology (JMEST), 6*(2), 74. https://doi.org/10.17977/um016v6i22022p074

Tura, A. D., Lemu, H. G., & Mamo, H. B. (2022). Experimental Investigation and Prediction of Mechanical Properties in a Fused Deposition Modeling Process. *Crystals, 12*(6), 844. https://doi.org/10.3390/cryst12060844

Ulkir, O., Ertugrul, I., Ersoy, S., & Yağımlı, B. (2024). The effects of printing temperature on the mechanical properties of 3D-printed acrylonitrile butadiene styrene. *Applied Sciences, 14*(8), 3376.

Xie, J., Sun, L., & Zhao, Y. F. (2025). On the Data Quality and Imbalance in Machine Learning-based Design and Manufacturing—A Systematic Review. *Engineering, 45*, 105-131. https://doi.org/10.1016/j.eng.2024.04.024

Yangue, E., Ye, Z., Kan, C., & Liu, C. (2023). Integrated deep learning-based online layer-wise surface prediction of additive manufacturing. *Manufacturing Letters, 35*, 760-769. https://doi.org/10.1016/j.mfglet.2023.08.108

Zhang, Y., Yang, S., Dong, G., & Zhao, Y. F. (2021). Predictive manufacturability assessment system for laser powder bed fusion based on a hybrid machine learning model. *Additive Manufacturing, 41*, 101946. https://doi.org/10.1016/j.addma.2021.101946

Zhou, L., Miller, J., Vezza, J., Mayster, M., Raffay, M., Justice, Q. …Bernat, J. (2024). Additive Manufacturing: A Comprehensive Review. *Sensors, 24*(9), 2668. https://doi.org/10.3390/s24092668

Zihao, X., Hongyuan, W., Pengyu, Q., Weidong, D., Ji, Z., & Fuhua, C. (2022). Printed Surface Defect Detection Model Based on Positive Samples. *Computers, Materials & Continua, 72*(3), 5925-5938. https://doi.org/10.32604/cmc.2022.026943

Biographies

JAYSON FRANCOIS is an adjunct professor in the Electrical Engineering Technology Department at Florida A&M University and a PhD candidate in the Electrical and Computer Engineering Department in the FAMU-FSU College of Engineering. He received his BS in computer engineering and his MS in electrical engineering from Florida A&M University. He has extensive experience with specialized materials in additive manufacturing, high voltage measurements and instrumentation, and artificial intelligence applications in the transportation and construction industry. Mr. Francois is a Dwight D. Eisenhower Transportation Research Fellow, an NNSA Path Scholars Fellow, and a GEM National Consortium Full Fellow. Mr. Francois may be reached at jayson1.francois@famu.edu

SHONDA BERNADIN is a Google-endowed full professor in the Department of Electrical and Computer Engineering in the FAMU-FSU College of Engineering. Dr. Bernadin received her BS in Electrical Engineering from Florida A&M University, her MS in Electrical and Computer Engineering from the University of Florida, and her PhD in Electrical Engineering from Florida State University. Her research interests include speech and image processing, data analysis, natural language processing, artificial intelligence, acoustic sensor integration, and semiconductor manufacturing and technologies. She is also very active in engineering education and outreach programs that seek to broaden engineering talent in the STEM workforce. Dr. Bernadin may be reached at bernadin@eng.famu.fsu.edu

INSTRUCTIONS FOR AUTHORS: MANUSCRIPT FORMATTING REQUIREMENTS

The INTERNATIONAL JOURNAL OF ENGINEERING RESEARCH AND INNOVATION is an online/print publication designed for Engineering, Engineering Technology, and Industrial Technology professionals. All submissions to this journal, submission of manuscripts, peer-reviews of submitted documents, requested editing changes, notification of acceptance or rejection, and final publication of accepted manuscripts will be handled electronically. The only exception is the submission of separate high-quality image files that are too large to send electronically.

All manuscript submissions must be prepared in Microsoft Word (.doc or .docx) and contain all figures, images and/or pictures embedded where you want them and appropriately captioned. Also included here is a summary of the formatting instructions. You should, however, review the sample Word document on our website (http://ijeri.org/formatting-guidelines) for details on how to correctly format your manuscript. The editorial staff reserves the right to edit and reformat any submitted document in order to meet publication standards of the journal.

The references included in the References section of your manuscript must follow APA-formatting guidelines. In order to help you, the sample Word document also includes numerous examples of how to format a variety of scenarios. Keep in mind that an incorrectly formatted manuscript will be returned to you, a delay that may cause it (if accepted) to be moved to a subsequent issue of the journal.

1. **Word Document Page Setup:** Two columns with ¼" spacing between columns; top of page = ¾"; bottom of page = 1" (from the top of the footer to bottom of page); left margin = ¾"; right margin = ¾".

2. **Paper Title:** Centered at the top of the first page with a 22-point Times New Roman (Bold), small-caps font.

3. **Page Breaks:** Do not use page breaks.

4. **Figures, Tables, and Equations:** All figures, tables, and equations must be placed immediately after the first paragraph in which they are introduced. And, each must be introduced. For example: "Figure 1 shows the operation of supercapacitors." "The speed of light can be determined using Equation 4:"

5. **More on Tables and Figures:** Center table captions above each table; center figure captions below each figure. Use 9-point Times New Roman (TNR) font. Italicize the words for table and figure, as well as their respective numbers; the remaining information in the caption is not italicized and followed by a period—e.g., "*Table 1*. Number of research universities in the state." or "*Figure 5*. Cross-sectional aerial map of the forested area."

6. **Figures with Multiple Images:** If any given figure includes multiple images, do NOT group them; they must be placed individually and have individual minor captions using, "(a)" "(b)" etc. Again, use 9-point TNR.

7. **Equations:** Each equation must be numbered, placed in numerical order within the document, and introduced—as noted in item #4.

8. **Tables, Graphs, and Flowcharts:** All tables, graphs, and flowcharts must be created directly in Word; tables must be enclosed on all sides. The use of color and/or highlighting is acceptable and encouraged, if it provides clarity for the reader.

9. **Textboxes:** Do not use text boxes anywhere in the document. For example, table/figure captions must be regular text and not attached in any way to their tables or images.

10. **Body Fonts:** Use 10-point TNR for body text throughout (1/8" paragraph indention); indent all new paragraphs as per the images shown below; do not use tabs anywhere in the document; 9-point TNR for author names/affiliations under the paper title; 16-point TNR for major section titles; 14-point TNR for minor section titles.

11. **Personal Pronouns:** Do not use personal pronouns (e.g., "we" "our" etc.).

12. **Section Numbering:** Do not use section numbering of any kind.

13. **Headers and Footers:** Do not use either.

14. **References in the Abstract:** Do NOT include any references in the Abstract.

15. **In-Text Referencing:** For the first occurrence of a given reference, list all authors—last names only—up to seven (7); if more than seven, use "et al." after the seventh author. For a second citation of the same reference—assuming that it has three or more authors—add "et al." after the third author. Again, see the *sample Word document* and the *formatting guide for references* for specifics.

16. **More on In-Text References:** If you include a reference on any table, figure, or equation that was not created or originally published by one or more authors on your manuscript, you may not republish it without the expressed, written consent of the publishing author(s). The same holds true for name-brand products.

17. **End-of-Document References Section:** List all references in alphabetical order using the last name of the first author—last name first, followed by a comma and the author's initials. Do not use retrieval dates for websites.

18. **Author Biographies:** Include biographies and current email addresses for each author at the end of the document.

19. **Page Limit:** Manuscripts should not be more than 15 pages (single-spaced, 2-column format, 10-point TNR font).

20. **Page Numbering:** Do not use page numbers.

21. **Publication Charges:** Manuscripts accepted for publication are subject to mandatory publication charges.

22. **Copyright Agreement:** A copyright transfer agreement form must be signed by all authors on a given manuscript and submitted by the corresponding author before that manuscript will be published. Two versions of the form will be sent with your manuscript's acceptance email.

    Only one form is required. Do not submit both forms!

    The form named "paper" must be hand-signed by each author. The other form, "electronic," does not require hand signatures and may be filled out by the corresponding author, as long as he/she receives written permission from all authors to have him/her sign on their behalf.

23. **Submissions:** All manuscripts and required files and forms must be submitted electronically to Dr. Philip D. Weinsier, manuscript editor, at philipw@bgsu.edu.

24. **Published Deadlines:** Manuscripts may be submitted at any time during the year, irrespective of published deadlines, and the editor will automatically have your manuscript reviewed for the next-available issue of the journal. Published deadlines are intended as "target" dates for submitting new manuscripts as well as revised documents. Assuming that all other submission conditions have been met, and that there is space available in the associated issue, your manuscript will be published in that issue if the submission process—including payment of publication fees—has been completed by the posted deadline for that issue.

    Missing a deadline generally only means that your manuscript may be held for a subsequent issue of the journal. However, conditions exist under which a given manuscript may be rejected. Always check with the editor to be sure. Also, if you do not complete the submission process (including all required revisions) within 12 months of the original submission of your manuscript, your manuscript may be rejected or it may have to begin the entire review process anew.

THE LEADING JOURNAL OF ENGINEERING, APPLIED SCIENCE, AND TECHNOLOGY

Print ISSN: 2157-8052
Online ISSN: 1930-6628

www.ijme.us

www.iajc.org

INTERNATIONAL JOURNAL OF MODERN ENGINEERING

ABOUT IJME:

- IJME was established in 2000 and is the first and official flagship journal of the International Association of Journal and Conferences (IAJC).
- IJME is a high-quality, independent journal steered by a distinguished board of directors and supported by an international review board representing many well-known universities, colleges and corporations in the U.S. and abroad.
- IJME has an impact factor of **3.00**, placing it among the top 100 engineering journals worldwide, and is the #1 visited engineering journal website (according to the National Science Digital Library).

OTHER IAJC JOURNALS:

- The International Journal of Engineering Research and Innovation (IJERI)
  For more information visit www.ijeri.org
- The Technology Interface International Journal (TIIJ).
  For more information visit www.tiij.org

IJME SUBMISSIONS:

- Manuscripts should be sent electronically to the manuscript editor, Dr. Philip Weinsier, at philipw@bgsu.edu.

  For submission guidelines visit
  www.ijme.us/submissions

TO JOIN THE REVIEW BOARD:

- Contact the chair of the International Review Board, Dr. Philip Weinsier, at philipw@bgsu.edu.

  For more information visit
  www.ijme.us/ijme_editorial.htm

INDEXING ORGANIZATIONS:

- IJME is indexed by numerous agencies. For a complete listing, please visit us at www.ijme.us.

Contact us:

Mark Rajai, Ph.D.

Editor-in-Chief
California State University-Northridge
College of Engineering and Computer Science
Room: JD 4510
Northridge, CA 91330
Office: (818) 677-5003
Email: mrajai@csun.edu

www.tiij.org

www.ijeri.org

IJERI

The International Journal of Engineering Research & Innovation (IJERI) is the second official journal of the International Association of Journals and Conferences (IAJC). IJERI is a highly-selective, peer-reviewed print journal which publishes top-level work from all areas of engineering research, innovation and entrepreneurship.

IJERI Contact Information

General questions or inquiry about sponsorship of the journal should be directed to:

Mark Rajai, Ph.D.

Founding and Editor-In-Chief

Office: (818) 677-5003

Email: editor@ijeri.org

Department of Manufacturing Systems Engineering & Management

California State University-Northridge

18111 Nordhoff St.

Room: JD3317

Northridge, CA 91330